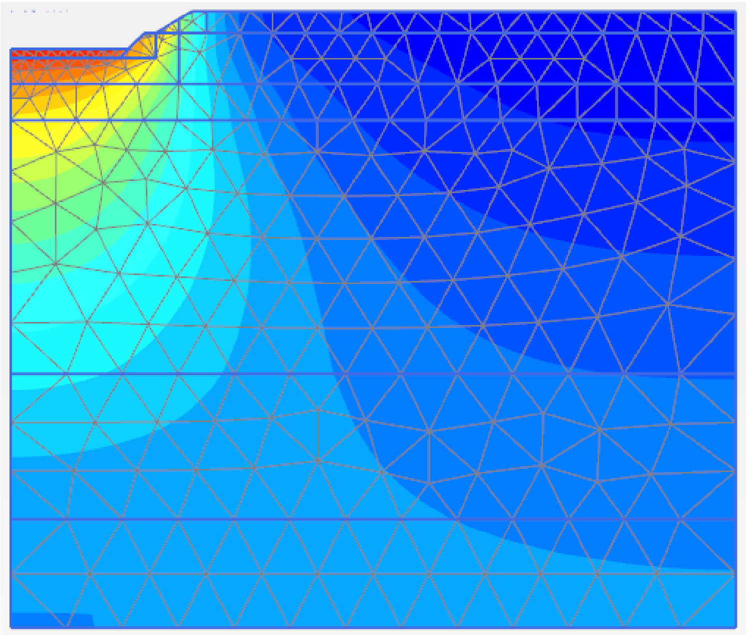

# Heave caused by excavation in soft soil

## A case study of a part of the Götatunnel project

Master's thesis in Infrastructure and Enviromental Engineering


RAMI ASADI
ELHAM SOKHANGO

Department of Architecture and Civil Engineering
CHALMERS UNIVERSITY OF TECHNOLOGY
Gothenburg, Sweden 2018

Master's thesis ACEX30-18-71

# Heave caused by excavation in soft soil

A case study of a part of the Götatunnel project


RAMI ASADI
ELHAM SOKHANGO


CHALMERS
UNIVERSITY OF TECHNOLOGY


Department of Architecture and Civil Engineering
*Division of Geology & Geotechnics*
Chalmers University of Technology



Master's thesis ACEX30-18-71
Gothenburg, Sweden 2018

Heave caused by excavation in soft soil
A case study of the Götatunnel project
RAMI ASADI
ELHAM SOKHANGO



Supervisor: Johannes Tornborg, Department of Civil and Environmental Engineering
Examiner: Mats Karlsson, Department of Civil and Environmental Engineering

Master's Thesis 2018:71
Department of Architecture and Civil Engineering
Division of Geology & Geotechnics
Chalmers University of Technology
SE-412 96 Gothenburg
Telephone +46 31 772 1000

Cover: Visualization of displacements obtained due to excavation, modelled in PLAXIS 2D.

Typeset in LaTeX
Gothenburg, Sweden 2018

Heave caused by excavation in soft soil
A case study of the Götatunnel project
RAMI ASADI
ELHAM SOKHANGO
Department of Architecture and Civil Engineering
Division of Geology & Geotechnics
Chalmers University of Technology

# Abstract

Numerical modelling is adapted to solve among other things, complex geotechnical problems. During excavation, the bottom of the excavation tends to heave caused by the reduction of total stress. Following thesis presents results of a comprehensive study on heave of a part of Götatunnel constructed through clay in Gothenburg, Sweden. The section is used as reference object for the analysis of heave caused by unloading using the finite element method for geotechnical analysis, PLAXIS 2D.

Several material models capturing the behaviour of soil based on assumptions are available. In order to analyze heave with regards to time, the Soft soil creep model is used of which the total strain is distinguished by a partly elastic- and visco-plastic part, taking creep effects into account. Analysis are conducted to validate if the the material model is able to capture unloading situations such as excavations. Provided laboratory data from the reference project has been evaluated and further analytical calculations has been derived to estimate the expected heave and how it is affected by unloading modulus. The obtained parameters are further subjected to calibration using numerical modelling in both compression and extension to resemble more accurate and reliable behaviour of the soil.

Results showed a difference between the unloading modulus obtained by the analytical and numerical modelling. The analytical formula which considers vertical effective stress and pre-consolidation pressure showed a lower modulus than the modulus obtained from the numerical analysis. The numerical modelling indicated a lower amount of heave than the heave measured on field. The numerical modelling does however not take account for the heave obtained during installation of piles, but takes account for consolidation processes which on the other hand is not obtained from field measurements. It came to conclusion that the material model Soft Soil Creep is not appropriate to use for unloading problems since it failed to capture the stress path of the extension as well as dissipation of the pore pressure. A more advanced material model, incorporating the anisotropy, small-strain stiffness and creep becomes relevant to pursue a result resembling more accurate behavior of the soil during unloading.

Keywords: Unloading, Soft soil, Clay, Numerical modelling, Unloading modulus, Swelling, Heave

# Acknowledgements

We would like to express our sincere gratitude to our supervisor Johannes Tornborg and examiner Mats Karlsson, for their encouragement and contribution with expertise throughout the work. By their support, motivation and inspiration we have been able to develop our knowledge in the field.

Lastly we would like to express our gratitude to our families and friends who have been by our side during the whole process.

Rami Asadi & Elham Sokhango, Gothenburg, June 2018

# Contents

# Nomenclature

**Abbreviations**

| | |
|---|---|
| $MC$ | Mohr coulomb |
| $OCR$ | Over consolidation ratio |
| $SS$ | Soft soil |
| $SSC$ | Soft soil creep |

**Greek letters**

| | |
|---|---|
| $\kappa^*$ | Modified swelling index |
| $\lambda^*$ | Modified compression index |
| $\mu^*$ | Modified creep index |
| $\nu'$ | Poisson's ratio |
| $\phi$ | Internal friction angle |
| $\psi$ | Dilatancy angle |
| $\sigma$ | Total stress |
| $\sigma'$ | Effective stress |
| $\sigma'_c$ | Pre-consolidation stress |
| $\sigma'_h$ | Effective horizontal stress |
| $\sigma'_o$ | Initial effective stress |
| $\sigma'_v$ | Effective vertical stress |
| $\sigma_f$ | Normal stress on the failure plan |
| $\tau_f$ | Shear strength |

**Roman letters**

| | |
|---|---|
| $a_s$ | Swelling index |
| $c$ | Cohesion |
| $E$ | Young's modulus |
| $M_{ul}$ | Unloading modulus |
| $p'$ | Mean effective stress |
| $q$ | Deviatoric stress |
| $s'$ | Average effective stress |
| $t$ | Maximum shear strength |
| $u$ | Pore water pressure |
| $u_e$ | Excess pore water pressure |
| $u_s$ | Static pore water pressure |

# List of Figures

# List of Tables

# 1

# Introduction

## 1.1 Background

Development of transportation infrastructure is essential with an increase of population, expansion and densification of urban areas. Densification of urban areas entails complexities with construction in historic city centers, which to some extent might require deep excavation followed by underground construction. In order to decrease construction time and project costs with maintained safety level, knowledge about soil response during unloading is of great importance. In Sweden, there are currently no standardized approaches or guidelines for management of the consequences of heave entailed by unloading of soil. This could be due to a need for research in this area and that it previously in Sweden has been studied less, in comparison to studies of the behavior of clay during aspects such as loading and settlements. Unloading of soil does not only affect the soil behavior in the short-term, e.g. construction period, but may also affect the soil behavior in the long-term performance, e.g. serviceability, of the construction. Therefore, it is of great interest to increase knowledge and account for the effects caused by unloading. Within the work of this thesis, the behavior of soft clay during unloading is analyzed, with the excavation for the construction of a part of the Götatunnel, located in Gothenburg Sweden, used as reference project.

## 1.2 Objective & Aim

The aim of this Master thesis is to analyze how deformation within and surrounding excavations is affected by unloading, time and how the use of a material model that incorporates viscous effects might predict the obtained deformations. The analysis should include an effective stress based model describing the unloading modulus dependence of effective stresses with regards to prevalent conditions during the construction of a part of the Götatunnel, in Gothenburg. The objective is to draw conclusions concerning:

- Can an effective stress based analysis using the constitutive model, Soft soil Creep, which incorporates viscous effects be used to simulate the ground movements and dissipation of pore water pressure that was measured during excavation for a section of the Götatunneln?
- Is it possible to model and analyze the long term behavior and performance

of ongoing and future creep settlements caused by unloading of an deep excavation using the software PLAXIS 2D?
- Is the equation for the unloading modulus presented in Trafikverket (2016) relevant in consideration of used constitutive model and conducted research?

## 1.3 Limitations

Simplifications has been made in order to study following subject using numerical modelling.

- Installation of hammered concrete piles in soft clay can cause excess pore water pressure as well as deformations and heave in areas adjacent to the pile installation area. According to Persson (2004) installation of concrete piles in the adjacent area affected the measurement results to some extent, for the excavation at the Götatunnel. Effects of pile installation prior to excavation has however not been included in the conducted analysis but has been taken in account during the discussion of the results.
- Heave or swelling caused by change of chemical properties (i.e. oxidation) and water content is not accounted for within the frame of this thesis.

# 2

# Characteristics of soil during unloading

Along with increased urbanization with requirements of sustainable development and effective demands of transport systems, more infrastructural projects are developed and constructed in soft soil. Underground construction projects including tunneling and building with basements or garages will to some extent require an excavation. To understand the behavior of the soil during excavation process, this chapter will present some relevant characteristics and behavior of soft soil.

## 2.1 Characteristics of soft soil

Excavation of soil causes disturbance to the in-situ soil equilibrium which if not addressed correctly, would affect temporary and permanent constructions as well as the surroundings (Knappett & Craig, 2012). According to Knappett and Craig (2012), soil consists mainly of soil grains with enclosing voids of compressible air and/or incompressible water. Due to the rearrangement of the three-phased soil distribution the behavior of the soil is affected because of changed particle position e.g. loading and unloading of the soft soil during dissipation of water. Usually, the prominent behavior of soil is distinguished and classified into two main modes of behavior: Undrained and drained behavior. The essential distinction of the two modes is if the excess pore pressure, created as a result of either loading or unloading, has dissipated or not. The undrained behavior is usually referred to as a short-term behavior where the created excess pore pressure has yet not dissipated. Furthermore, the long-term case is obtained when the excess pore pressure has dissipated, this case is referred to as a drained. To understand and therefore predict achieved strength and bearing capacity of soil, the complexity of soft soil is important to understand, as it depends on the apparent behavior. Fredlund and Hasan (1979) describes by the use of Terzaghi's one dimensional consolidation theory the cause of the transition between the two phases as a change of effective stresses. Fredlund and Hasan (1979) further states that the applied stresses initially, during a short-term case, is transmitted through the water affecting the total stress that transmits to changes in effective stress during a long-term case. The interparticle forces acting between the soil grains in soft soils is related with the water pressure according to equation 2.1

$$\sigma' = \sigma - u \tag{2.1}$$

The formula above describes the effective stress as the difference between total stress and pore water pressure. The applied load to saturated soft soil is primarily conveyed by the water and subsequently alters to be carried by the soil grains only. This stress, conveyed by the soil skeleton is denoted as the effective stress (Knappett & Craig, 2012).

## 2.2 Pore pressure

The effective stresses mentioned in the previous paragraph, is found to be affected by the pore water pressure. The pressure of the water filling the voids, enclosing the soil particles is described as pore water pressure, u, presented in the formula below as the sum of the static- and excess pore water pressure. The static pore water pressure, $u_s$, defined as the constant value, is affected by the position of the water table. Depending on if the change in total stress refers to a load or unloading situation, delay of water seepage causes the pore water pressure to increase or decrease from the static value. This pressure is known as, excess pore water pressure, $u_e$ and the change is equal to the change in total stress (Knappett & Craig, 2012).

$$u = u_s + u_e \tag{2.2}$$

When loading or unloading soil, a variation in pore pressure influencing the effective stresses will occur. The excess pore pressure caused by unloading of soil during excavation will dissipate with time and is according to Knappett and Craig (2012) affected by the permeability, stiffness and drainage conditions of the soil.

By application of Terzaghis's one dimensional consolidation theory, it is assumed that the application of vertical stress is initially carried by the pore water hence, developing excess pore pressure (Kempfert & Gebreselassie, 2006). The excess pore pressure will dissipate over time causing changes in vertical stress and therefore rearrangement of the soil particles will occur. However, since the water in the voids is incompressible, such rearrangement could not take place until the water is able to dissipate (Knappett & Craig, 2012). The load will finally be transferred through the soil particles along with a volume change. The time dependency depends mainly on the drainage conditions and permeability of the soil and will along with the dissipation cause one dimensional vertical deformation according Terzaghi's consolidation theory.

Knappett and Craig (2012) mentions that below the water table, also defined as phreatic level, the soil is saturated and the pore pressure is positive. The pore pressure in the saturated soil above the water table will be negative. The negative pore pressure i.e. suction, is affected by the permeability of the soil hence the height of which the pore water pressure diffuses e.g. capillary rise differs between soil type. The decreased total vertical stress during excavation causes initial reduction of pore pressure, resulting in induced negative excess pore pressure during excavation in soft soil. Yu-qi, Hong-wei, and Kang-he (2005) explains how the development of the negative excess pore pressure could trigger a process resembling the reverse of consolidation. This will follow by a consequence of swelling due to gradual increase of volume of the soil (Knappett & Craig, 2012). Yu-qi et al. (2005) means that the initial stress field in the soil is changed during excavation, and that the consequences because of dissipation of excess pore pressure, such as decrease of effective stresses causing a reduction of strength, may cause an increased load effect to for example to the retaining structures

## 2.3 Bottom heave due to unloading

In vicinity of excavations, the surrounding area will withstand an increased risk of settlements, unlike the bottom of excavation where heave may develop. Knappett and Craig (2012) for example describes the phenomenon heave during excavation caused by high difference in hydraulic gradients at opposite side of the retaining structure. According to (Knappett & Craig, 2012) and (Friis & Sandros, 1994), the development of heave caused by unloading can be an effect of several factors and can be described as an inverted consolidation process. For heave to occur, the saturated soil must allow water flow, causing volume change. Knappett and Craig (2012) describes bottom heave because of unloaded soil mass, of which an upward movement of the excavation bottom tend to occur. This phenomenon induced by a decrease of the effective stresses caused by unloading hence, the soil behind the retaining walls tend to push the soil of the excavation bottom upward.

Due to unloading of the soil e.g. excavation, the in-situ soil is as mentioned in previous paragraph, subjected to changes. The change resulting in a reduction in total stress eventually causes water intake from the surrounding area hence, a volume change of the voids. Initially, the pore water pressure is decreased and a negative excess pore pressure will occur. As the pore water pressure progressively increases to the static pressure, heave will gradually develop.

Zeevaert (1983) highlights that development of heave can be categorized in four main categories, with different driving forces. The different categories are presented as; Elastic heave, driving heave, Swelling heave and Plastic heave and are described below, with elastic heave being the focus in this thesis.

1. Elastic heave: Taking place during excavation is caused by the reaction of the clay material to unload stress relief.
2. Swelling heave: Considers upward time-dependent movement in expansive clay minerals caused by presence of swelling clay minerals. Due to water intake as result to stress relief caused by excavation, the soil may heave caused by swelling.
3. Plastic heave: bottom failure resulting in upward movement due to the ratio between the shear stress and shear strength.
4. Driving heave: Upward movement of the soil caused by disturbance of the soil

when driving piles into the soil.

Eurocode 7 states that the different mechanisms potentially causing heave should be analyzed before construction. In order to withstand displacements of the structure, deformation and loss of function of the soil, the serviceability limit state design criteria need to be fulfilled (EN, 1997). The limit state design is compiled in EN (1997) Eurocode 7 which represents three causes of heave during unloading which should be considered, with the first two criterion's implementable within the aim of the following thesis.

1. Heave caused by a reduction of effective stresses
2. Heave caused by constant volume conditions in fully saturated soil, thus causing settlement of contiguous structures
3. Settlement of the adjacent structures

## 2.4 Unloading modulus

Several methodologies and developed formulas exist for calculation of heave, raised as a consequence of unloading which is of importance for predicting the amount of heave empirically. Based on conducted research and laboratory testing of soil several empirical relations have been identified by various of scholars such as: Larsson (1986), (Karlsrud & Hernandez-Martinez, 2013) and Persson (2004). Larsson (1986) who studied the unloading modulus using results from oedometer tests mentions that the unloading modulus is dependent of the stress and highlights observations obtained during laboratory tests and describes the stress dependent unloading modulus, compiled in equation 2.3. Larsson (1986) indicates that the unloading modulus is higher for stresses closer to the pre-consolidation pressure. This is due to secondary compression e.g. creep for stresses close to the pre-consolidation pressure. The unloading modulus will decrease with decreasing stress as a result of decrease creep rate and unloading of soil however, at stresses greater than 80 percent of the pre-consolidation stress, heave will not occur due to the development of secondary swelling.

$$M_{ul} = \frac{\sigma'_v}{a_s} \tag{2.3}$$

Where,
$M_{ul}$ = Unloading modulus
$\sigma'_v$ = Vertical effective stress
$a_s$ = Swelling index, 0.01 for swedish clays

Further studies were made by for example (Karlsrud & Hernandez-Martinez, 2013) who compared different methods and observed the impact of the unloading modulus, pre-consolidation pressure and unloading. Karlsrud and Hernandez-Martinez (2013) concluded that the stiffness is related to not only the pre-consolidation pressure and the stress level of the soil, but also the magnitude of the unloading which is compiled in the formula below.

$$M_{ul} = 250\sigma'_v(\frac{\sigma'_v}{\sigma'_c - \sigma'_v})^{(0.3)} \tag{2.4}$$

Where
$\sigma'_v$ = Vertical effective stress
$\sigma'_c$ = Pre-consolidation pressure

Persson (2004) presented field and laboratory measurements from the Götatunnel as basis for the calculated unloading modulus. The unloading modulus conferred in the research as a part of Götaleden, is compiled by equation 2.5.

$$M_{ul} = 1500\sigma'_c(\frac{\sigma'_v}{\sigma'_c})^4 \tag{2.5}$$

The Swedish transport administration has created a compilation of geotechnical standards e.g. TR Geo 13. According to the following technical description, the unloading modulus for slightly over consolidated soils is presented by equation 2.6, Trafikverket (2016) which is based on the concluded equation of unloading modulus by (Persson, 2004):

$$M_{ul} = 10\sigma'_c e^{5(\sigma'_0/\sigma'_c)} \tag{2.6}$$

Tornborg (2017) pointed out that, since equation 2.6 from Trafikverket (2016) is based on the research by Persson (2004), the $\sigma'_0$ in equation 2.6 should be $\sigma'_v$ since the unloading modulus is determined by the current vertical effective stress level.

As seen in figure 2.1 , the unloading modulus varies depending on which formula is used. As noted, the unloading modulus according to Larsson (1986) changes direction when the load reduction becomes very large. Heave will not be developed at stresses greater than $0.8\sigma'_c$ since secondary swelling starts to develop.

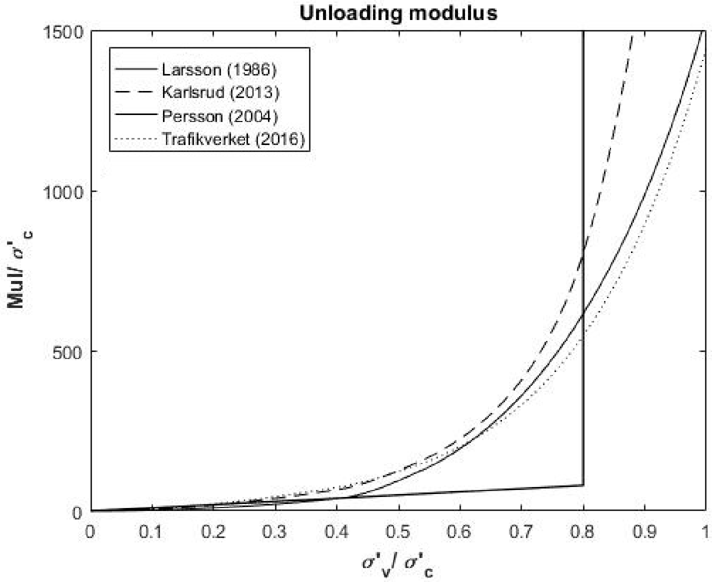


**Figure 2.1:** Distribution of different unloading modulus

## 2.5 Stress path during unloading

Kempfert and Gebreselassie (2006) emphasizes the importance of considering the state of a stress point whether it is unloading, reloading or primary loading since the deformation of the soil is stress path dependent.

The behavior of soil during unloading conditions has been subjected to research by for example Yuan and Nguyen (2011), emphasizing the importance of knowledge regarding this subject as the chosen stress path may induce plastic strains leading to failure. A way of visualizing the present stress state of a sample during testing is by plotting the Mohr-Coulomb circle. But as different stress states is continuously obtained during triaxial testing it is often more convenient to plot points representing the top of each circle, see figure 2.2. The connected points known as the stress path are thereby not unique as they are highly dependent of the stress state subjected to the sample.

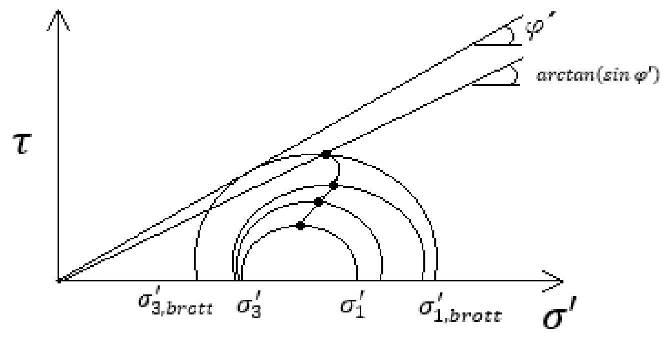


**Figure 2.2:** Visualization of the stress path during a consolidated-undrained triaxial compression test (Infrastruktur, 2005)

Considering an excavation presented in figure 2.3, the major principle stress may be reduced at the bottom of the excavation while the minor principle stress in the direction of the plane strain will be reduced adjacent to the slope of the excavation followed by a minor change in major principle stress (Zhang, Zhang, Li, & Shi, 2011). Research presented by Mesri, Ullrich, and Choi (1978) states that during unloading, the relation between the effective horizontal stresses and the vertical stresses could increase to an extent causing development of passive failure zones. By performance of an triaxial extension test it is possible to expose a soil sample to such stress states, and thus identifying the soil response. An example of such is presented in figure 2.3 by s'-t plot, whereas the average effective stress is denoted as *s'* and the shear strength as *t*.

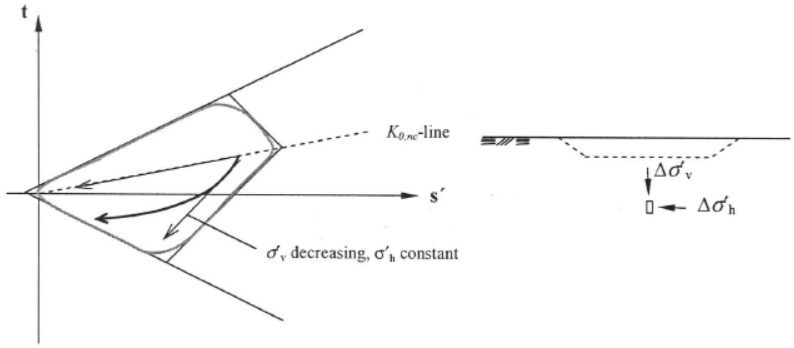


**Figure 2.3:** Idealization of a stress path obtained by performance of triaxial extension test (Persson, 2004)

## 2.6 Stiffness and deformation of soft soil

As stress path dependency is an important aspect regarding the appearing soil behavior it can be stated that parameters such as yield strength, friction angle and shear modules varies depending on the stress path and geotechnical application (Yuan & Nguyen, 2011). Since soft soil is governed by characteristics such as non-linear, plastic and anisotropic behavior (Persson, 2004), the choice of material model in numerical analysis does not always cover such behavior in act of simplification. However, it should be noted that usage of a linear-elastic material model is only justified for small strain conditions. A common distinction between the models is often represented by the applied stress- strain relationship, see figure 2.4, where the extent of the elastic region is governed by the pre-consolidation pressure.

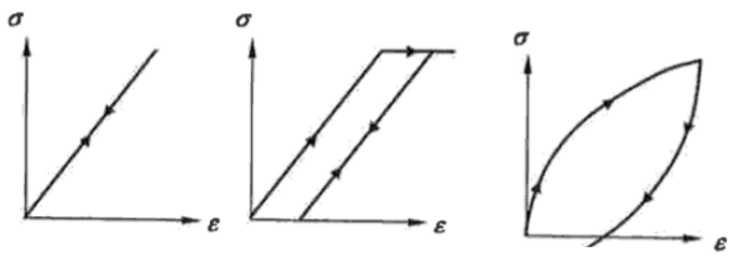


**Figure 2.4:** Examples of stress-strain relationships of different material models a) linear elastic model, b) elastic-perfectly plastic model, c) nonlinear model (Persson, 2004)

## 2.7 Small strain stiffness

By incorporation of small strain stiffness, it is assumed that the stress range from which the soil is able to recover almost completely is very small (R. B. Brinkgreve et al., 2017). The stiffness of soil is thereby assumed to relate to strain by non-linearity at rates far below the range obtained at end of construction, see figure 2.5.

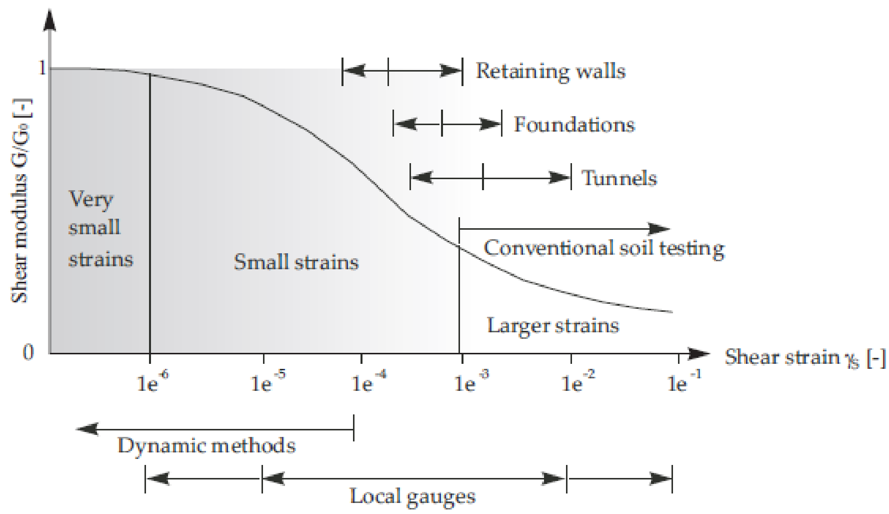


**Figure 2.5:** The behaviour of stiffness with increased strain (R. B. Brinkgreve et al., 2017)

Implementation of small strain stiffness is made by relating the variation of stiffness with strain, in terms of initial shear modulus, $G_0$ which describes the behavior of both drained and undrained condition, and shear strain level, $\gamma_s$ (Wood, 2016). By ignoring small strain behavior, an overestimation of strains and underestimation of load effects in geo-constructions, as retaining walls, are obtained. Wood (2016).

## 2.8 Anisotropy of soil

Due to forming processes affecting the stratification of the soil grains, the soil could exhibit a degree of anisotropy. Although conventional testings of soil considers isotropic shear strength, the natural soil is anisotropic. Assouline and Or (2006) explains that the anisotropy of soil is characterized by the transport properties of the soil for example, the flowing volume of fluid through porous area. Assouline and Or (2006) emphasizes that the anisotropy has a great impact on the prediction of flow, and that it plays a significant role in applications such as slope stability and bearing capacity of deep foundations (Won, 2013). Wood (2016) concluded in the report that among other things, the anisotropy of the soil is of great importance as basis for numerical analysis thus, capturing more reliable behavior of the soil. The constitutive material model soft soil explained further in chapter 3, considers isotropic behavior in both extension and compression which is not necessarily the case in general.

Most of the clay minerals tend to deposit with the flat soil structure down. Furthermore, the hydraulic conductivity affected by the soil anisotropy differs between the vertical and lateral direction depending on the soil structure (Zaslavsky & Rogowski, 1969). During different stress conditions, different undrained shear stress is obtained for different directions. According to (Won, 2013) the anisotropy of clays decreases as the plasticity index increases. The plasticity index describes the water content for which the soil has a plastic consistency. The anisotropic strength is described by the ratio of undrained shear strength in extension and compression. The lower anisotropy, the higher anisotropic strength.

## 2.9 Expansive clay

The characteristics of expansive clay is that the volume increases, i.e. swells, when allowing water inflow, and shrinks when water is withdrawn (Basma, Al-Homoud, Malkawi, & Al-Bashabsheh, 1996). In order to avoid potential damages to constructions in soil containing expansive clay, swelling phenomenon need to be addressed. The clay of the southwest part of Sweden is of glacial and post glacial marine origin deposited in salt water. According to Rankka et al. (2004) the dominating clay mineral in Sweden is the non-swelling Illite. The structure of the clay mineral consists of a gibbsite sheet between two sheets of silica. The combined sheets are linked with non-exchangeable Potassium ions. The Gibbsite sheet is compiled by a hydroxyl ion shard with octahedral unit, see figure 2.6. Silica sheet of which is enclosed by two gibbsite sheets, is formed by oxygens shared with tetrahedral unit. The volume change caused by swelling is mainly affected by the clay mineral montmorillonite. The clay mineral has the same structure as Illite however, the sheets are bonded by water molecules. When potential water adsorbs between the combined sheets of montmorillonite, swelling occurs (Knappett & Craig, 2012).

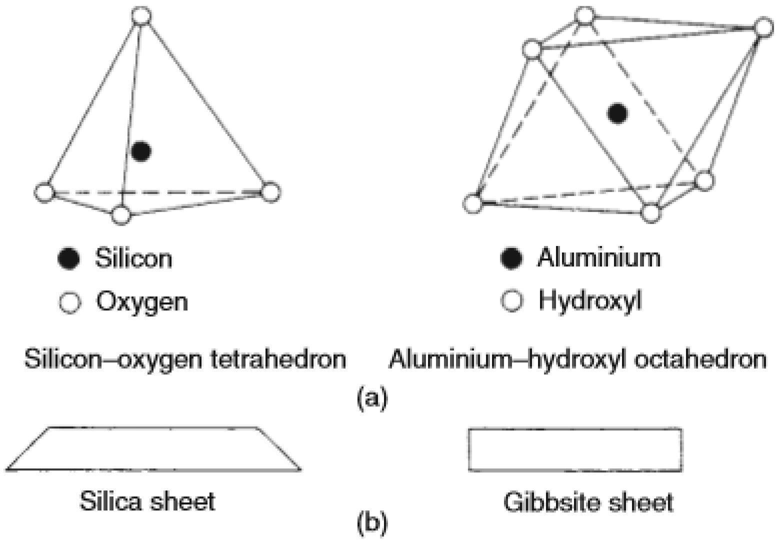


**Figure 2.6:** Visualization of silica and gibbsite mineral respectively (Knappett & Craig, 2012)

# 3
# Numerical modelling

In order to analyze the heave of the deep excavation, the finite element based program PLAXIS 2D version 2017 is used. The program with a broad range of features is used for applications in geotechnical and civil engineering. The excavation is modelled using the software in order to obtain realistic assessment of displacements and stresses using different calculation types. A range of constitutive models can be used in PLAXIS hence, the behavior of different material is allowed to be simulated (R. Brinkgreve & Vermeer, 1998).

## 3.1 Constitutive material models

Numerical modeling is largely based on approximations, where constitutive relationships are implemented to reflect the natural behavior of the soil. The material models used are all based on different assumptions and the result obtained can thus be retrieved with different deviations. Such approximations have been presented by R. B. Brinkgreve et al. (2017) and Runesson, Steinmann, Ekh, and Menzel (2006) to name a few, stating that the assumptions that the different material models are based on can differ significantly. A usual fundamental difference between the models constitutes the stress strain relationship, as shown in figure 3.1. R. B. Brinkgreve et al. (2017) presents several material models weaknesses and strengths are highlighted. Mohr Coulomb was presented among them representing a rough approximation and not at all considered the most optimal partly due to its stress-strain relationship (see Figure 3.1a) compared with more advanced models. Although, this might be evident, in modeling a balancing must be done as advanced models may entail other complexities. R. B. Brinkgreve (2005) addresses in his report, the problem behind this and explains that complex models impose higher demands on the input and require that certain factors are estimated. In section 3.1.1-3.1.2 a selection of material models are exposed for evaluation as relevant basis for the objectives of this thesis report.

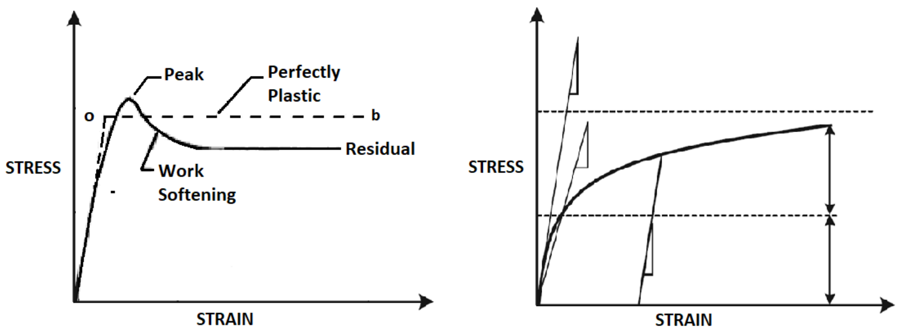


**Figure 3.1:** Stress strain relationship of the left figure, a) Elasto-perfectly plastic/-Mohr Coloumb. And the right figure b) Hyperbolic/Hardening soil (Schanz et al., 1999)

### 3.1.1 Mohr Coulomb

Mohr Coulomb is presented by Jia (2018) as mainly suitable for rough estimations, since the model is based on assumptions that limits the real mechanical behavior of soil. The model is described as an elastic-perfectly plastic model, where both the elastic and plastic intervals are linear (see Figure 3.1a). Jia (2018) explains that Mohr Coulomb is based on a combination of two relationships (i.e Hooke's law and Coulomb's law) where the elastic region is mainly represented by two essential variables, namely the Young's modulus (E) and Poisson's ratio (v'). The plastic region, representing the irrecoverable deformations, is mainly governed by the stress state defined by Mohr Coulomb's failure criteria (see equation 3.1). Thus, further two variables appear, i.e. the friction angle ($\phi$) and cohesion (c).

$$\tau_f = c + \sigma_f tan\phi \tag{3.1}$$

As equation 3.1 represents the failure envelope it becomes evident that failure will be obtained in case of development of any critical combination of the shear stress and effective normal stress, and thus plastic deformations will be obtained. As soil can be subjected to different stress states it should be noted with reference to the figure 3.2 that possible combination of shear stress and effective normal stress can only result either under or on the failure envelope. Thus, a stress state falling above the failure envelop, presented in figure 3.2 is not possible. Furthermore, a stress state fulfilling the failure criteria (intersecting the failure line) will emphasize the perfectly behavior assumed by the model, and thus cause plastic strains causing irrecoverable deformations.

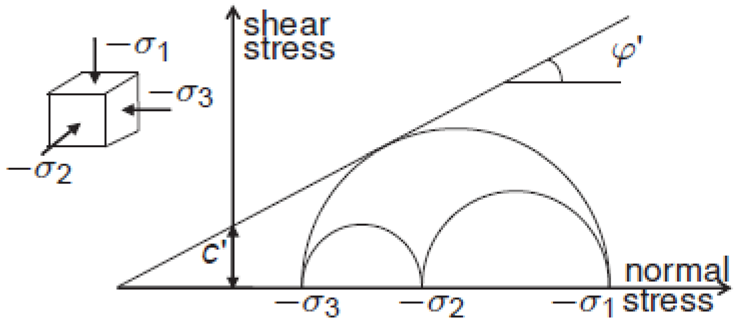


**Figure 3.2:** Failure envelope of Mohr Coulomb (R. B. Brinkgreve et al., 2017)

Irrecoverable volume changes due plastic strains is also covered by the model, thus by the definition of the dilatancy angle, $\psi$, (Ti, Gue See, Huat, Noorzaei, & Saleh, 2009, p. 93), which controls the development of plastic strains.

## Limitations

The simplicity of the model is considered to generate an effective tool for an initial first order approximation of the response of clay with only a few parameters required. Thus, it should be noted that the soil model does not incorporate behavior such as strain and stress dependency nor the anisotropic behavior of soft soil. The model assumes a simple elastic perfectly plastic stress-strain relationship and can thereby not estimate accurate behavior of soil as different characteristics dominates depending on if the soil is subjected to un-/reloading or loading. Furthermore, the approximations conducted is also based on an average stiffness parameter obtained for each soil layer, which is independent of the type of activity (i.e. primary loading, un-/re-loading). The application of constant stiffness parameters limits the reliability of the outcome and is a further reason behind why it's classified as first order approximation. Additionally, the lack of yield surface decreases the applicability of the model as implementation of a dilatation value, may cause unrestricted shearing with constant volume for some cases.

### 3.1.2 Soft Soil

R. B. Brinkgreve et al. (2017), categorizes the Soft Soil material model amongst the advanced ones, although the Soft soil model is based on isotropy. But despite an isotropically basis the material model has its advantages, such as hyperbolic relation of stress-strain relationship during primary loading, distinction between primary- and un-/re-loading, memory for pre-consolidation and stress dependent stiffness (R. B. Brinkgreve et al., 2017). The yield surface is represented by an ellipse, whereas possible stress states are restricted by Mohr Coulomb failure criterion. Hence, it is not possible to account for strain softening. Karstunen and Amavasai (2017) presents this as a strict limitation of the applicability as such characteristics is essential to cover significant behavior of soft soil. Furthermore, it is not possible to obtain a stress state outside the yield surface, due to a defined consistency condition. Stress states can thereby only be achieved either inside or on the yield surface.

By implementation of Mohr Coulombs failure criterion, the critical state parameter M is no longer implemented for failure cause. Thus, the M* parameter is implemented instead for shape adjustment of the ellipse, and defines the height of the ellipse, see figure 3.3. By implementation of this factor for such because it is possible to manipulate the shape of the yield surface. Hence, obtainment of reasonable values of the coefficient of lateral earth pressure (K0-value) at normally consolidated region can be ensured (Karstunen & Amavasai, 2017).

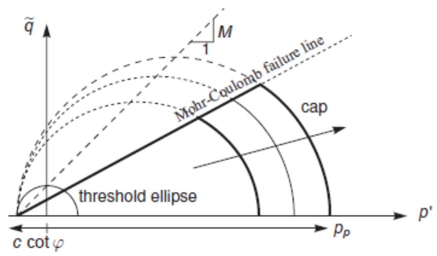


m

**Figure 3.3:** Yield surface - Soft Soil model. (R. B. Brinkgreve et al., 2017)

## Soft Soil Creep model

The Soft Soil Creep model, denoted as SSC, is mainly based on the Soft Soil model, thus with extensions including time dependency and strain rates.

### One-dimensional creep

Based on research led by Buisman (1936), it was discovered that classical consolidation theory was not sufficient to explain soft-soil settlements and implementation of a creep law was therefore suggested (Vermeer & Neher, 1999). This has later been subjected to research by various scholars; for example, Mesri (1977), Garlanger (1972), Bjerrum (1967), all states that total strain should be further distinguished by partly an elastic- and partly visco-plastic part.

A distinctive characteristic of the creep models is the possibility of achieving stress states outside the yield surface, and hence OCR<1 is obtained describing the state of the soil. Karstunen et al. (2006) states that such stress conditions is mainly caused by inter-particle bonding, posing as a resistance against yielding and the compression curve will thereby converge against the intrinsic compression line as bonding are gradually being destroyed by developed creep strains, see figure 3.4.

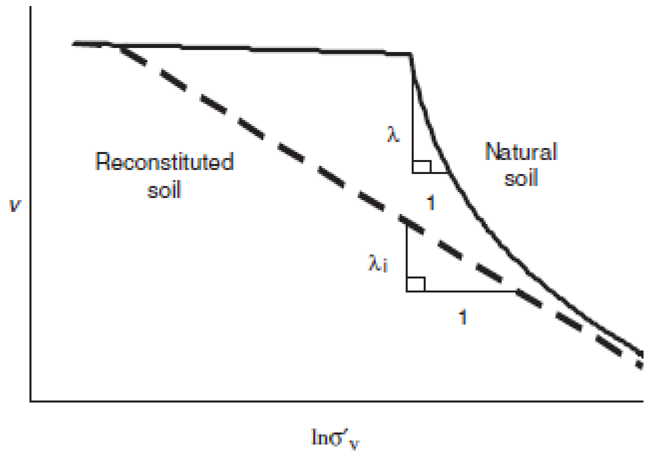


**Figure 3.4:** Oedometer curves obtained from tests on natural and reconstituted soil (Karstunen et al., 2006)

The position of the yield curve, is initially determined by the pre-consolidation stress. Unlike the soft soil model, it is determined by a function of time. The pre-consolidation surface, represented by the yield curve, is therefore initially only considered as a reference surface since the new state will not be obtained instantaneously. The reference time is set as 1 day in the SSC model, representing the time of which the compression curve will have reached the normal consolidation line during a oedometer test (Vermeer & Neher, 1999).

The expansion velocity and the location of the curve in the stress space are the two parameters that should be accounted for in the SSC model. According to Waterman and Broere (2004) These are entered by means of the over consolidation ratio, OCR and the modified creep index. Moreover, the change of the creep rate is described by the combination of the modified creep index $\mu^*$, modified swelling index, $\kappa^*$ and modified compression index, $\lambda^*$

# 4

# Study area - Case Study Götatunneln

The Götatunnel is located in central Gothenburg and was constructed during the period of 2000-2006 as a part of the project "Götaleden". Some parts of the project were studied during excavation, for example, a part labeled "L3" was studied by Persson (2004). This thesis is mainly based on laboratory results and field measurements conducted during the period of her research. The tunnel was mainly constructed through rock with respective passage of the tunnel constructed through clay. A section through the latter material is focused in this thesis.

## 4.1 Geology and historic development

The area of interest is the construction site (L3, see figure 4.1) situated close to Lilla Bommen, in a region called Gullbergsvass. In the early 19th century, the region was characterized by wetland. The environment within this area has suffered drastic changes over time as demand for suitable land to build on is continuously increasing. Parts of the wetland had been dried out and imposed with piles and filled up, with gravel and sand, in level with surrounding environment, after which they were built on (Sweco, 2014).


**Figure 4.1:** Location of study area, L3 (Jonsson & Kristiansson, 2004).

## 4.2 Geotechnical properties

Geotechnical data provided from laboratory tests of soil samples were mainly obtained from two boreholes, see figure 4.2. Ground conditions of the studied section is further interpreted and presented in this section. The soil samples collected from borehole A and B were subjected to oedometer and CRS tests. However, the triaxial test results are based on soil samples collected approximately 100m south of borehole B.

An analysis of the pre-consolidation pressures compared to the in-situ stresses (prior to excavation) indicates that the clay is normally consolidated to slightly over consolidated. The analysis was based on evaluation of CRS tests obtained from borehole B for various of depths, which resulted in a OCR of 1.8 in the top layer after which it decreases linearly to 1.3 at 40 meters depth. This differs from statement and test results from Persson (2004), whom indicated an OCR of 1.1.

To estimate the heave caused by unloading of the excavation, the parameters given from respective test were evaluated and used to obtain additional empirically derived geotechnical parameters.

As samples from the investigated location are presented, the soil profile is characterized by the unit weight, water content and sensitivity of the soil, see figure 4.3. The soil has been divided into 5 layers consisting of fill overlaying 4 layers of clay.

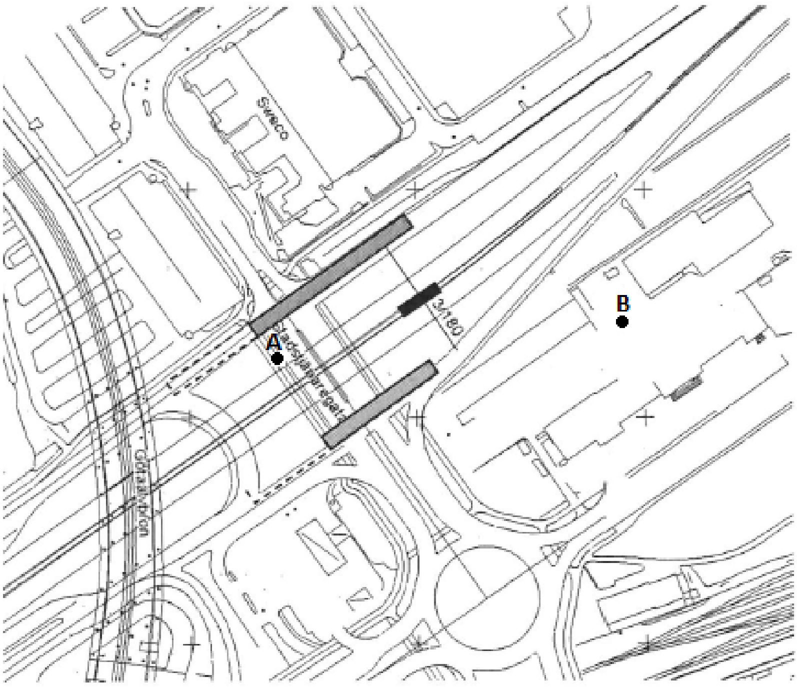


**Figure 4.2:** Map from Persson (2004) complemented with location of boreholes and indication of section 3/180 studied by Persson (2004)

## 4.3 Soil stratigraphy

The top 25 meters of the soil is evaluated using two boreholes (Point A and B), see figure 4.2. However, soil properties at deeper levels has only been evaluated using borehole B. Although borehole B is not located at the construction site, it is representable since soil within the area of Gullbergsvass obtains similar geological history and similar properties can therefore be found in the area in general.

Within the study area presence of clay through the soil profile is dominant. Based on field investigations the depth of fill has proven to vary within the range of 2,5-3 meters (Sweco, 2014). PM Geoteknik presented by Sweco further presents a possible division of the present fill material by two layers, of which the upper layer (1), reaching between 1-2 meter below ground, are mainly characterized by coarser material (e.g. stone, sand and gravel) followed by a lower layer (2), represented by clay and silt, characterized as dry crust. The fill layers appear as homogeneous with an underlying layer of normally consolidated to slightly over consolidated soft clay reaching as far as 100 meters of depth at most.

Since properties has proven to vary through the soil profile, the variation of characteristics of the soil is captured by division of the profile in layers. The division is based on three types of laboratory test procedures: CRS, oedometer and triaxial test and is presented in figure 4.3- 4.4.

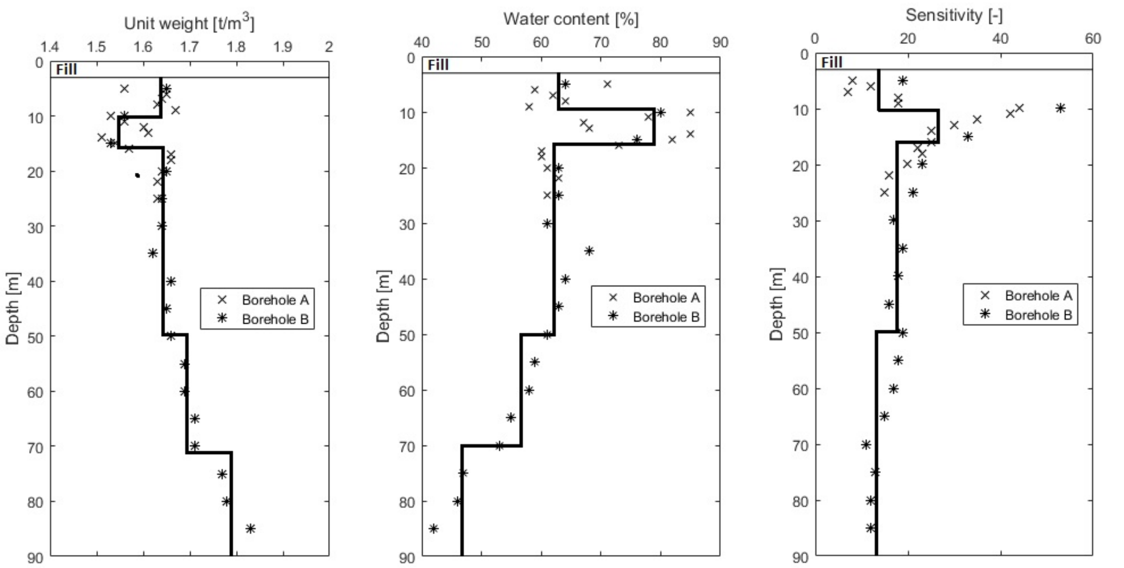


**(a)** Unit weight **(b)** Water content **(c)** Sensitivity

**Figure 4.3:** Characterization of soil profile

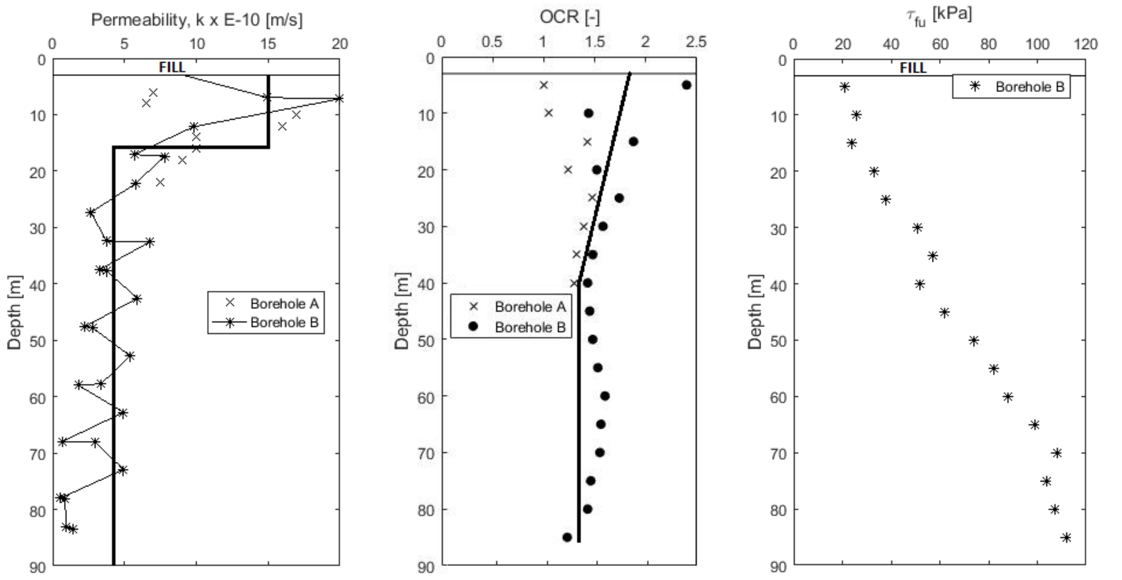


**(a)** Permeability

**(b)** OCR

**(c)** Undrained shear strength

**Figure 4.4:** Properties of the soil

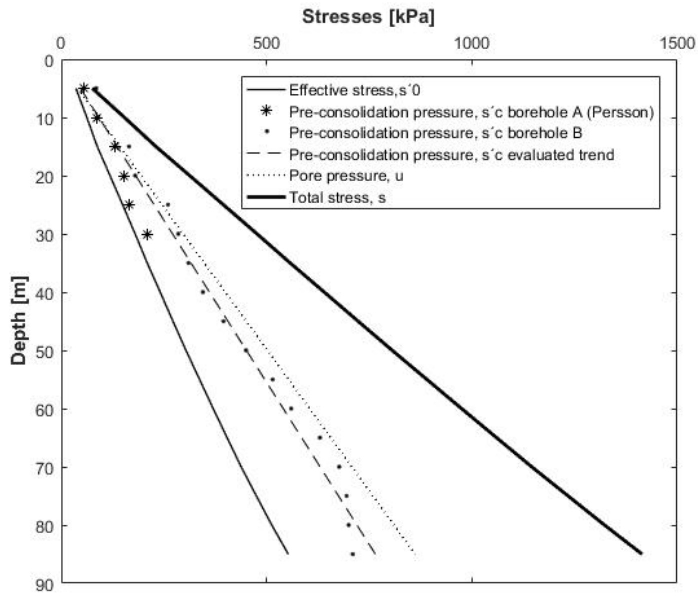


**Figure 4.5:** Stresses and pore pressures distribution of the chosen section

The obtained data from laboratory tests regarding stresses and pore pressure distribution from the reference project is compiled in figure 4.5 starting from the excavation bottom. As can be seen, the evaluated pre-consolidation pressure is presented as a combination of the pre-consolidation from the field of borehole A and

B respectively. The evaluated OCR presented in 4.4b shows an OCR of 1.8 for the first meters which may be a high value compared to 1.1 presented by Persson (2004). This is mainly based on the laboratory tests obtained from borehole B since pre-consolidation for greater depths are not presented by Persson (2004) for more reasonable evaluations. The reason for the difference in OCR, may be a result of the chosen density of the soil which is lower than obtained by Persson combined with older and disturbed samples which is used as basis for the conducted research.

## 4.4 Results from field measurements at Götatunneln part L3

The deep excavation of the Götatunnel was performed through two stages conducted during a period of approximately three months respectively. During the first excavation stage, the soil was excavated down to a depth of 3 meters. The open cut of excavation bottom was filled with 20 cm of gravel. The soil during the second stage was further excavated to a depth of 6.4 m, followed by filling of 1.2 m of macadam to ensure stability.

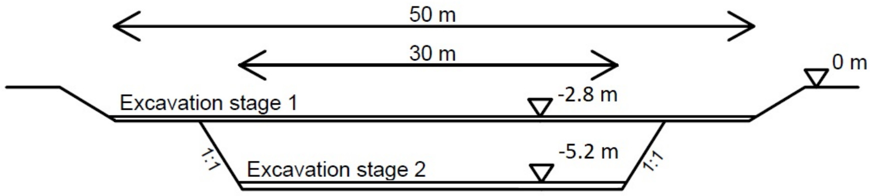


**Figure 4.6:** Cross-section of the excavation

By placement of extensometers, heave gauges, piezometers and earth pressure cells development of heave, pore pressures and horizontal stress relief were measured continuously during construction. The results are presented in figure 4.7-4.8 with clearer figures presented in A.2-A.4. What can be noted is the almost instant uplift obtained during the time of excavation. By comparison of development of heave and pore pressure over time (see figure 4.7), coinciding changes appears in both figures at equivalent time in both figures. As expected, negative excess pore pressure is developed instantly, followed by dissipation of the negative excess pore pressure. Heave is thereby obtained and increase with the equalization of the pore pressure.

Measurement of the horizontal total pressures indicates a major stress relief during excavation. The increase of the horizontal earth pressure during consolidation, shown in figure 4.8, is ruled by dissipation of negative pore pressure, which is clearly shown in figure 4.7b.

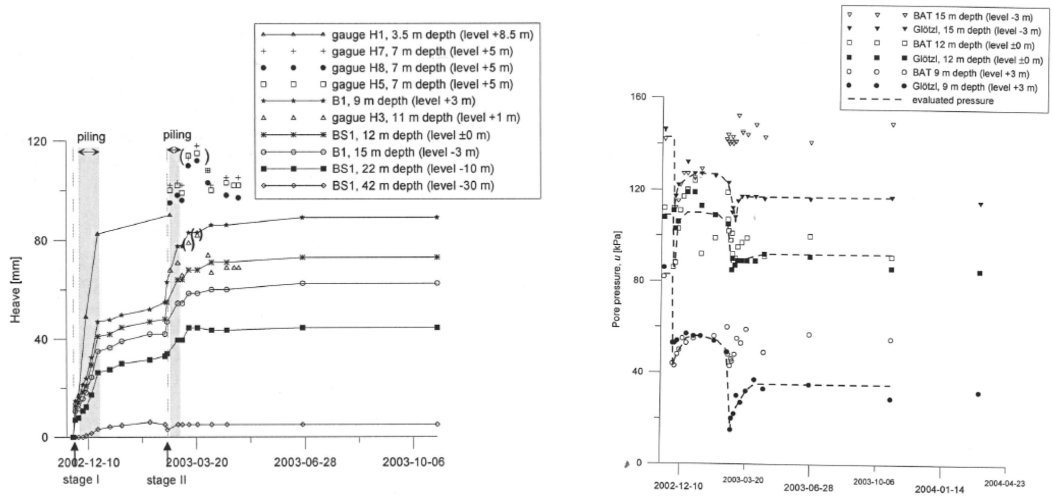


**(a)** Obtained heave at different depths

**(b)** Pore pressure during construction

**Figure 4.7:** Obtained data from field measurements (Persson, 2004)

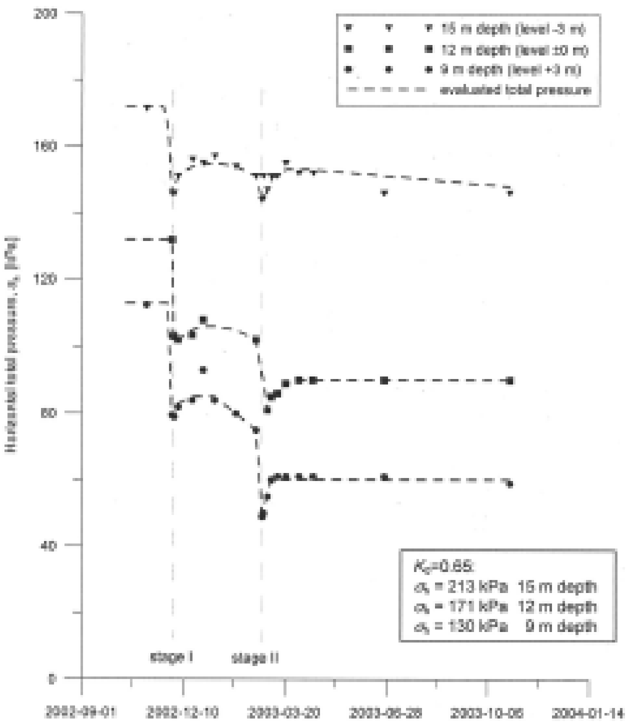


**Figure 4.8:** Changes in horizontal earth pressure during construction (Persson, 2004)

# 5

# Analysis

When performing a geotechnical analysis, an evaluation of soil parameters obtained from the laboratory testing is necessary. Following chapter initially presents a procedure for derivation of an analytical estimation of expected heave, followed by a method behind the derivation and evaluation of the soil parameters, contributing as basis for numerical analysis set up. In order to capture the elastic - visco plastic behavior of the soil, the Soft soil creep model was used. This is furthermore followed by a presentation of the methodology used for the numerical model set-up.

## 5.1 Analytical analysis

An analytical estimation is initially derived and aims to estimate the expected heave obtained due to unloading. The analysis is only considered a rough estimation of the expected heave, in order to set guidelines of the expected magnitude of heave from the numerical analysis using Plaxis. Thus, the obtained heave due to piling, in the results from Persson (2004), is not distinguished in the analysis. Furthermore, influence due to boundaries are neglected, that is the shear stresses and/or mobilized slope stability against the sides of the excavation. The calculations are simplified based on reversed consolidation theory and follows procedures similar to an example presented by Tornborg (2017).

### 5.1.1 Calculation procedure

The condition of the excavation is divided in three categories; Pre excavation ($t_0$), Post excavation ($t_{+0}$) and infinite time post excavation ($t_{inf}$). The ground water table is located at a depth of 1.1 meter below ground level and increases hydrostatically. The soil is homogeneous clay with a unit weight of $16.5kN/m^2$. The width of the excavation is assumed to be 30 meters, and reaches a depth of 6.4 meters, whereas the initial change in pore pressure, directly after excavation, is assumed to be derived according to equation 5.1. The assumption is based on field measurements obtained during the construction of the Tingstadstunnel located close to the examined area, which is presented in an analysis by (Alén & Jendeby, 1996).

$$\Delta u_{t+0} = 0.8\Delta\sigma_v \tag{5.1}$$

The change in total stress due to unloading is derived according to a 2:1 pressure distribution, presented in equation 5.2

$$\Delta\sigma_v = \frac{qb}{b+z} \tag{5.2}$$

The pore pressure at $t_{inf}$ is defined with reference to a research by Persson (2004), where measurements two years after the construction of the Tingstadstunnel indicate that the affected pore water distribution only reaches a depth of 35m. The steady state pore pressure ($u_{inf}$) is thereby defined with a starting point at excavation bottom and interpolated to match the initial pore pressure at 35 meters depth before excavation. The resulting states of pressure are presented in figure 5.1.

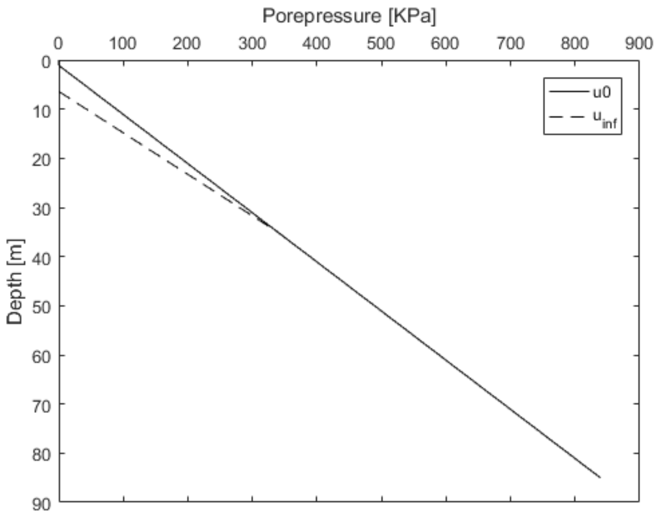


**Figure 5.1:** Assumed pore pressure distribution at $t_0$ and $t_{inf}$

The estimation of heave is thereafter conducted by reverse consolidation theory, whereas the unloading modulus is derived according to Trafikverket (2016), by equation 2.6

$$M_{ul} = 10\sigma'_c e^{5(\sigma'_v/\sigma'_c)} \tag{5.3}$$

The unloading modulus are later chosen based on the results presented in figure 5.2b and defined with reference to half the depth, where-after the development of heave is estimated by equation 5.4, see figure 5.3. Furthermore, a sensitivity analysis has been conducted on two parameters (permeability and modulus), and is also presented in figure 5.3.

$$Heave(t) = d\Big(\frac{\sigma'_0 - \sigma'_{t+0}}{M_{ul,1}} + \frac{\sigma'_{t+0} - \sigma'_{inf}}{M_{ul,2}}U\Big) \tag{5.4}$$

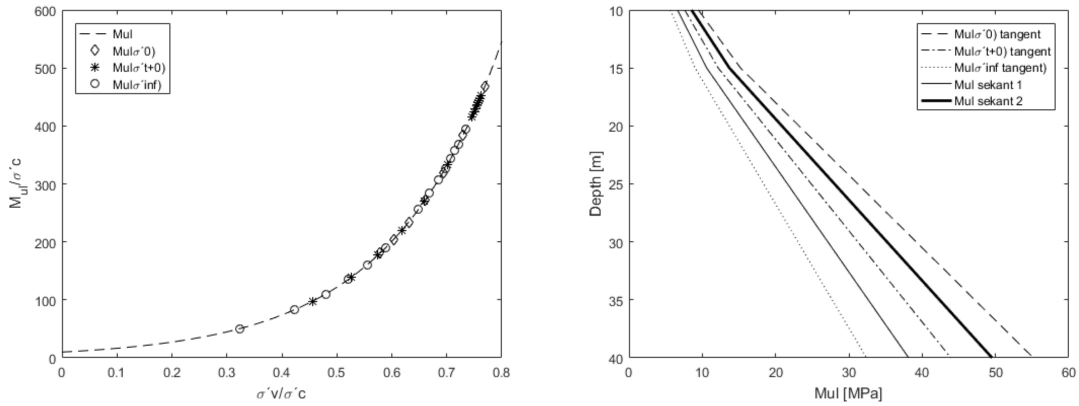


**(a)** Unloading modulus vs stress **(b)** Unloading modulus vs depth

**Figure 5.2:** Estimated modulus derived analytically

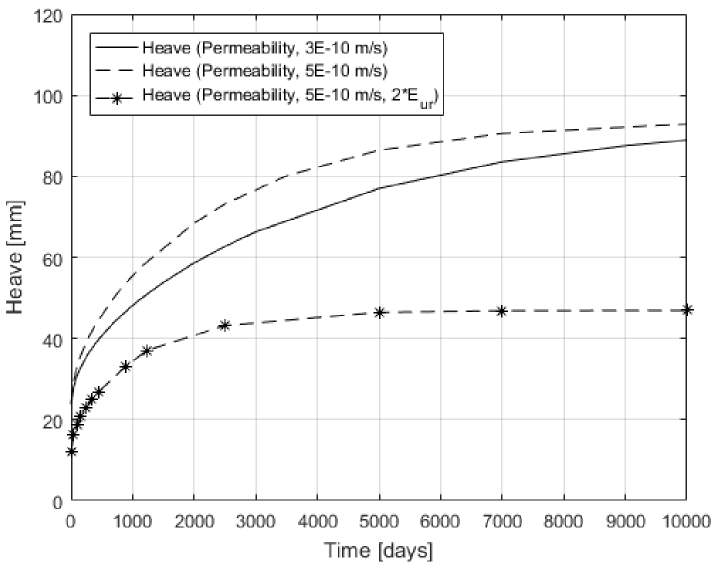


**Figure 5.3:** Development of heave approximated analytically

## 5.2 Parameter evaluation

The soil samples obtained from the two boreholes (see figure 4.2), were later subjected to stepwise oedometer, CRS and triaxial tests. Hence, parameters were derived in line with the procedures, presented by Karstunen and Amavasai (2017), from respective test:

- Triaxial compression and extension tests: Friction angle, Cohesion
- CRS : Pre-consolidation pressure, permeability, Modulus values
- Oedometer: Stiffness parameters ($\lambda$*,$\kappa$*) and modified creep index ($\mu*$)

By evaluation of triaxial tests, the friction angle and cohesion were obtained. However, the obtained values were considered too high and was therefore adjusted. The friction angle was thereby modified to 30 degrees, according to the guidelines of Trafikverket (2016), and a cohesion intercept of 1 kPa was initially chosen and later subjected to adjustments during calibration.

## Soft soil creep parameters

The soft soil parameters: modified swelling index, $\kappa^*$ and modified compression index, $\lambda^*$ can be obtained by the inclination in a ln p'-$\epsilon$ plot, as presented in figure 5.4a, according to the guidelines presented by Karstunen and Amavasai (2017).

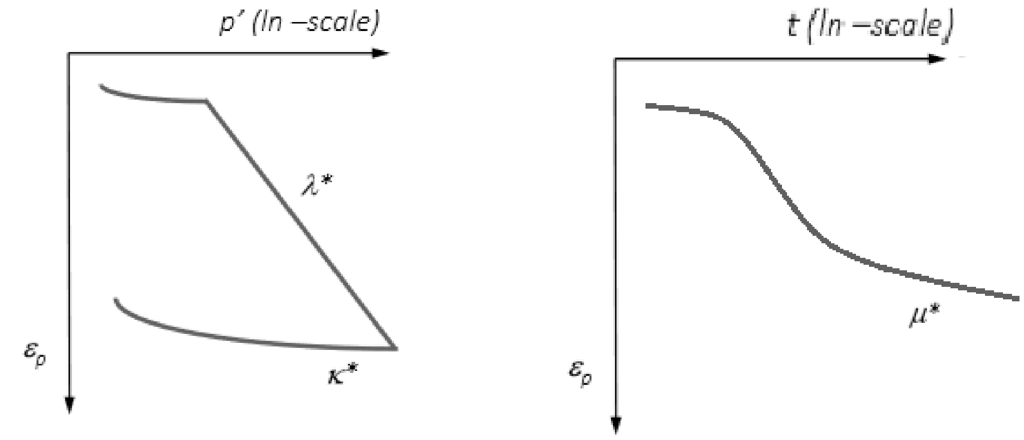


(a) Modified compression index, $\lambda^*$ and modified swelling index, $\kappa^*$

(b) Modified creep parameter, $\mu^*$

**Figure 5.4:** Derivation of soft soil creep parameters (Karstunen & Amavasai, 2017)

The creep parameter, $\mu^*$, was derived by an initial evaluation of oedometer creep tests for different strain levels, according to figure 5.4b. The evaluated parameters are thereafter plotted against the stress level for each creep test normalized by the effective vertical stress, as can be seen in figure 5.5. By normalizing the obtained creep parameters, it is possible to implement a consistency check for the parameters and to obtain a range in which the creep parameter may variate. The creep parameter was thereafter calibrated in order to resemble ongoing creep settlements in the area. The reference time parameter, $\tau_d$, is set equal to 1 day, further explained in Chapter 3.1.2.

As the aim of the report is to examine the unloading behavior of soil, emphasis was put on the evaluation of the modified swelling index, $\kappa^*$, and the creep parameter, $\mu^*$. The soil parameters were therefore subjected to adjustments for the chosen material model to resemble the soil behavior, in both the triaxial and oedometer tests in order to obtain results that are as good as possible. Further details regarding

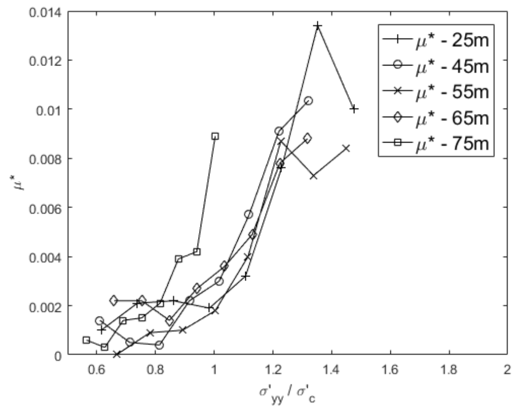


**Figure 5.5:** Creep parameters for various depths evaluated from borehole B, normalized with pre-consolidation pressure, $\sigma_c'$ obtained from CRS test.

the calibration are presented in Chapter 5.3 with calibrated soil layer parameters presented in Appendix: A.1

## 5.3 Parameter calibration

Manual evaluation of parameters from test results, in conjunction with simplifications and assumptions applied by different material models that are implemented in PLAXIS, can entail deviations causing non-representative and unreasonable behavior. The evaluated parameters were thereby considered as initial values and were further calibrated to resemble the test results obtained from the triaxial and oedometer tests, by implementation of the PLAXIS feature Soil test.
As the material models implemented in PLAXIS all assume different simplifications of the soil behavior (see Chapter 3), they resemble the real behavior with different accuracies. By calibration of the evaluated soil parameters, the aim is to fit the behavior obtained from the Soil test in PLAXIS to the results obtained from the real triaxial test: hence the sources of error can be minimized.

The calibration results presented in figure 6.3-6.4 and Appendix A are based on the chosen material model, Soft soil creep, implemented in the work of this thesis. It should be noted that more accurate models exist. However, with more advanced models further complexities are entailed. The possibility of resemblance of soil behavior is thereby restricted by the choice of material models. Nevertheless, it is not considered to limit the possibility of achieving the aim of the thesis. For further discussion on the impact the choice of material models, see Chapter 7.

## 5.4 Numerical modelling

### 5.4.1 Geometry of the model

The excavation was conducted during a period between 2002-2003 and was performed in two stages. Installation of conventional braced sheet piles was performed in connection to the excavation to prevent groundwater flow in the top soil layers. However, this is not taken in consideration during modelling in act of simplification. During the first stage, the soil was excavated to a depth of 3 meters followed by 20 centimeters of back-filling. The second stage of excavation was performed to a depth of 6.4 meters, followed by back-filling of 1.2 meters of macadam. Furthermore, since the construction is symmetrical, only half of the construction is modelled in PLAXIS.

As it is assumed that the soil and ground water relations remain the same across a wider area, the boundary conditions of the model, at the vertical boundaries, are closed: hence not allowing seepage of water. However, both horizontal boundaries remains open as the clay overlies a layer of friction material from which the state of ground water can recover. The groundwater table, located 1.1 meters below ground level, is model with a hydrostatic distribution. The excavation is modelled as "dry", hence not allowing seepage of water within the excavation area. The model size is set to 120 x 85 meters and is chosen with regards to minimization of influence due to boundaries conditions.

### 5.4.2 Model setup

In order to estimate the development of heave with regards to time, a material model which incorporates creep effects was chosen: Soft soil creep. The material parameters evaluated from soil tests obtained from Stadsbyggnadskontoret and from the adjacent project of Regionens hus were initially evaluated and calibrated according to procedures presented in chapter 5.2. Since the excavation was considered symmetrical, half of the excavation was modelled in PLAXIS 2D. The model extended from 0 - 100 m with a depth starting at 0 m and reaching a depth of -85 m. Soils with respective input and calibrated parameters were assigned to each layer obtained from the analysis from the laboratory tests, see table A.1 in appendix. The model was followed by a medium mesh with mesh refinement around the excavation area seen in the figure 5.6, followed by a convergence analysis in order to assure acceptable uncertainties in the result.

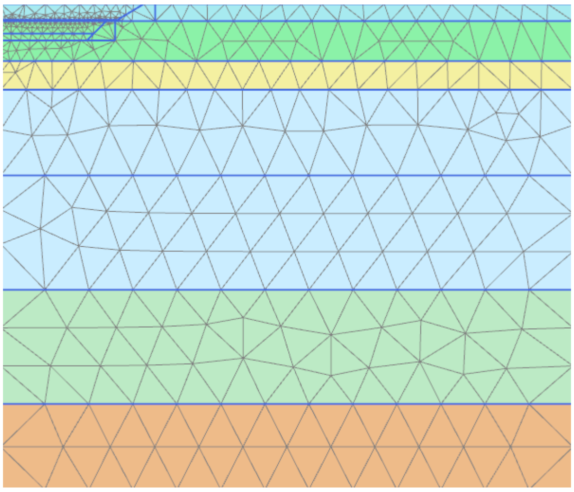

**Figure 5.6:** Geometry and mesh distribution of the excavation model

The model was thereafter set up in order to resemble the progress of construction, as presented by Persson (2004), and the stages are presented in table 5.1.

**Table 5.1:** Set of calculation steps implemented in PLAXIS 2D version 2017

| Phase | Calculation type | Loading type | Pore pressure | Time [days] |
|---|---|---|---|---|
| Initial | K0-procedure | Staged Construction | Phreatic | - |
| Excavation 1 | Plastic | Staged Construction | Phreatic | 3 |
| Consolidation 1 | Consolidation | Staged Construction | Use pressures from previous phase | 87 |
| Excavation 2 | Plastic | Staged Construction | Phreatic | 7 |
| Consolidation 2 | Consolidation | Staged Construction | Use pressures from previous phase | 90 |
| Consolidation 3 | Consolidation | Min. excess porepressure | - | - |

# 6

# Results

## 6.1 Evaluated parameters and comparison of model simulations

Based on laboratory results performed on samples from borehole A and B (see figure 4.2), the clay is divided into 5 layers. The division has mainly been ruled by variations in unit weight, and are presented in figure 4.3. Variations in water content, sensitivity and modulus is not considered as a dominant factor for division, however it is used as supportive measure of the chosen soil division. The soil parameters were obtained by evaluation of CRS, Oedometer and Triaxial tests. However, it should be mentioned that while CRS was evaluated for every fifth meter through the soil profile, triaxial and oedometer results were only evaluated for two depths (10 and 27 meters). Although triaxial- and oedometer tests were only evaluated for two depths, the division resulted in a total of 5 layers. This was because the evaluation of laboration result showed a change in density, water content and modulus that coincided with the presented layer division.

By calibration with reference to the behavior obtained during triaxial compression- and extension tests, the stress path of the soil when subjected to loading/unloading is captured, while CRS and oedometer test results resembles the stiffness the present soil appears with during loading in oedometric conditions. The results obtained by calibration with oedometer and CRS lab. results as reference are presented in figure 6.1-6.2.

**Table 6.1:** Calibrated soft soil creep parameters

| Layer | Depth [m] | $\lambda^*$ | $\kappa^*$ | $\mu^*$ |
|---|---|---|---|---|
| 1 | 3 - 10 | 0.16 | 0.023 | 0.0077 |
| 2 | 10 - 15 | 0.21 | 0.020 | 0.0079 |
| 3 | 15 - 30 | 0.22 | 0.013 | 0.0078 |
| 4 | 30 - 50 | 0.30 | 0.020 | 0.0071 |
| 5 | 50 - 70 | 0.22 | 0.017 | 0.0054 |

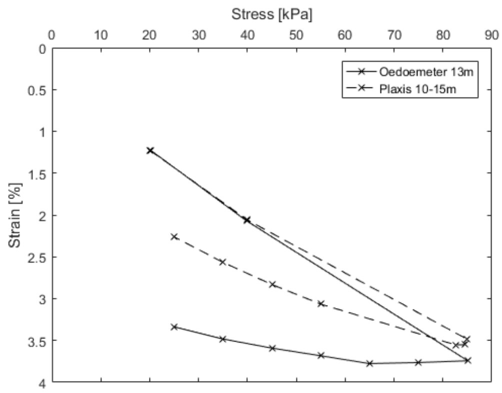


**(a)** 10m

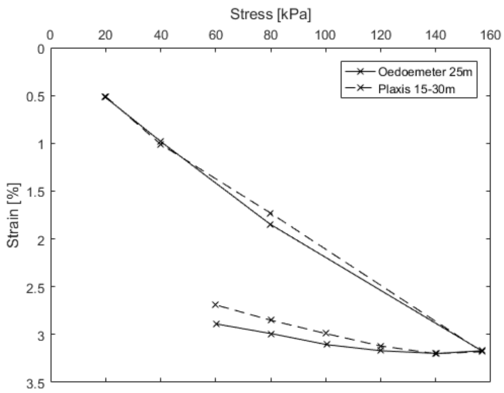


**(b)** 25m

**Figure 6.1:** Calibration with incremental load oedeometer test results, obtained from borehole B, as reference

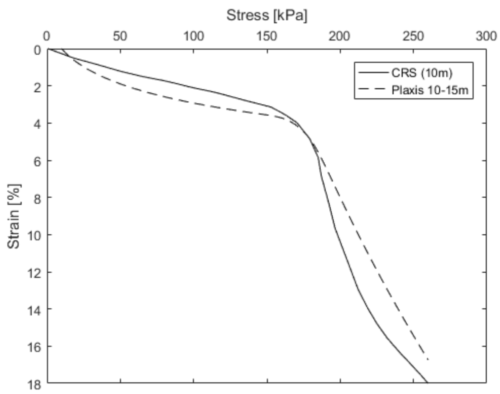


**(a)** 10m

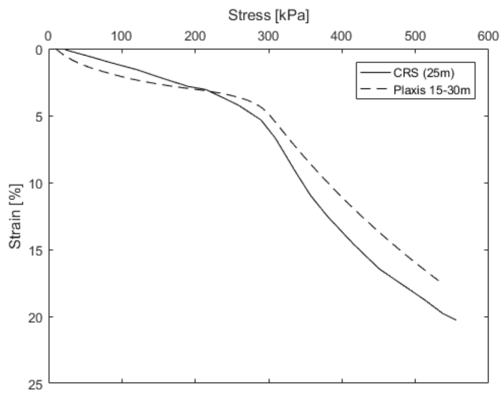


**(b)** 25m

**Figure 6.2:** Calibration with CRS test results, obtained from borehole B, as reference

The evaluated parameters obtained are further calibrated with triaxial compression- and extension tests as reference and are presented in figure 6.3 and 6.4 for two depths, where the stress invariants (p' and q), are defined as follows:

$$p' = \frac{\sigma_1 + \sigma_2 + \sigma_3}{3} \qquad\qquad q = \sigma_3 - \sigma_1$$

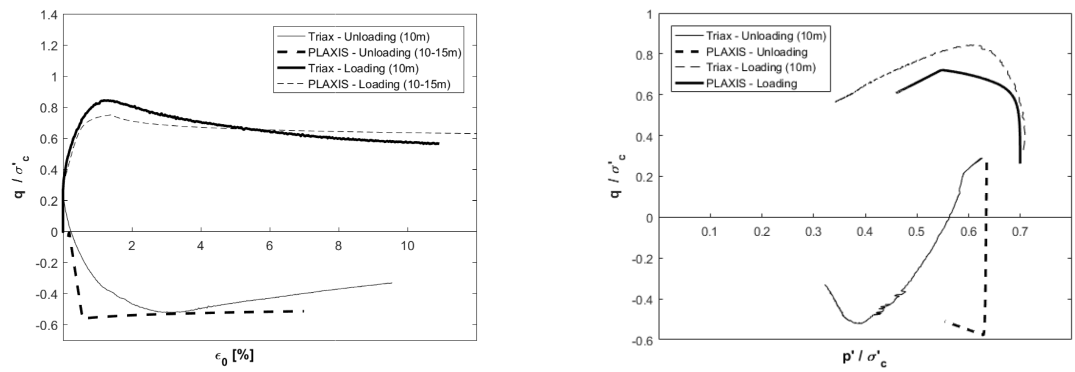


(a) Deviatoric stress, q, normalized with $\sigma_c'$ versus strain

(b) p'-q plot normalized by $\sigma_c'$

**Figure 6.3:** Calibration with triaxial test results, at 10m depth, as reference

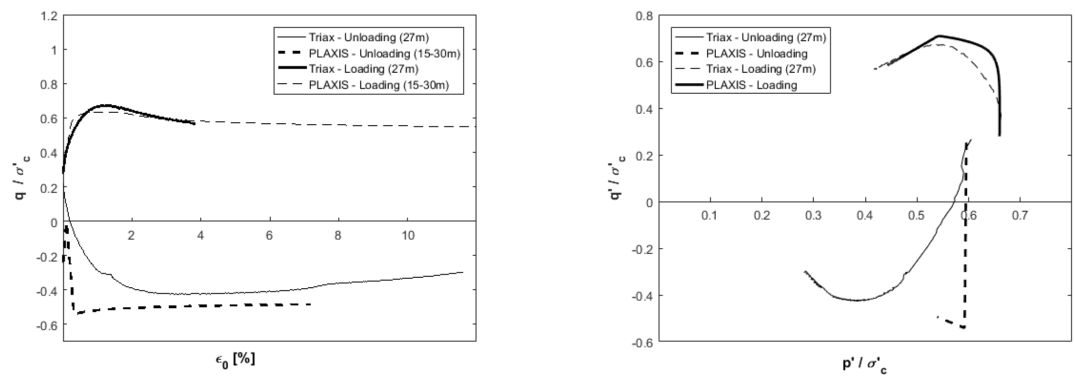


(a) Deviatoric stress, q, normalized with $\sigma_c'$ versus strain

(b) p'-q plot normalized by $\sigma_c'$

**Figure 6.4:** Calibration with triaxial test results, at 27m depth, as reference

## 6.2 Numerical modelling results

### Analytical versus numerical model

The numerical model conditions are validated against the assumptions for the analytical calculation, from which stress and pore pressure distribution at $t_0$, $t_{+0}$ and $t_{inf}$ are resembled. The stress states and pore pressure distribution during all three time periods are presented in figure 6.5. However, it should be highlighted that the excess pore pressure caused by unloading deviates in the top 30 meters of the soil. This is believed to be caused partly by a combination of that there is not as much negative pore pressure the first 30 meters and that the numerical modelling takes deformation into account so that the negative pore pressure drops directly after excavation. The software PLAXIS does not take the soil behavior for an infinite time after excavation in account hence, a tendency to stabilize and equalize the pore pressure causes the deviation of the pore water pressure.

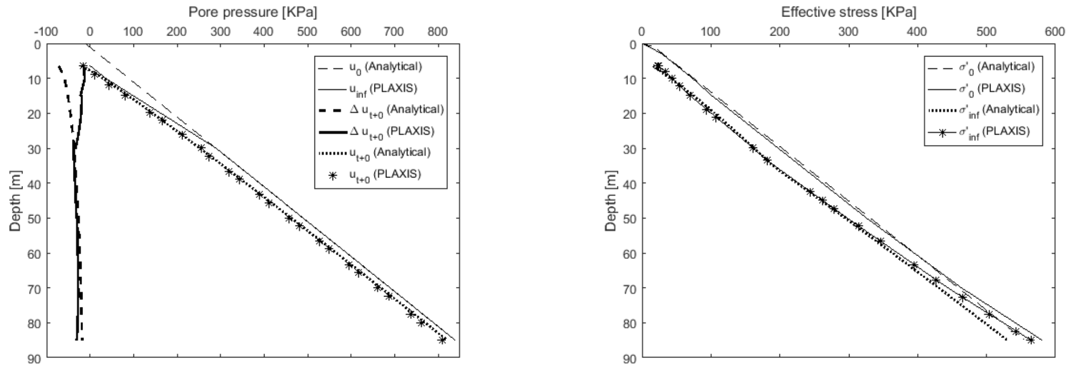


**(a)** Pore pressure distributions when unloading

**(b)** Effective stress distribution

**Figure 6.5:** Validation of PLAXIS model against analytical calculations

As presented in figure 6.6, the unloading modulus implemented in the analytical versus numerical model differs, and the numerical model implements a higher modulus value than the analytical model. The main reason for this deviation is that the analytical model derives the unloading modulus by means of vertical effective stress, $\sigma'_v$, and pre-consolidation pressure, $\sigma_c$, according to equation 2.6 presented by (Trafikverket, 2016). The material model, Soft soil creep, implemented in the numerical model, on the other hand derives the modulus by means of modified swelling index, $\kappa^*$, modified compression index $\lambda^*$ and modified creep index, $\mu^*$.

By setting the result obtained from the analytical model and the numerical model in relation, it can be seen that the initial heave obtained in the analytical model is higher than the obtained magnitude in the numerical model, see figure 6.7b. However, it should be clarified that the analytical calculation is based on an excavation corresponding to the total depth performed in one step, unlike the numerical where the excavation is performed in two stages with intermediate consolidation phases. Thus, it is not possible to set the instant heave, that can be seen in figure 6.7b in comparison. However, the development during the consolidation phases is compared. What is evident is that the evolution of heave separates the cases as the magnitude of heave obtained, in the analytical model, during consolidation is greater. The results presented in figure 6.7a was derived in order to compare the instant heave obtained during similar conditions. Figure 6.7a presents thereby results from an analytical model, thus representing the first excavation stage followed by three months of consolidation. The results indicate that a lower magnitude of heave is obtained when set in comparison with the numerical results. The numerical model takes into account deformations, contributing to positive excess pore pressure which counteracts the negative pore pressure resulting from unloading, continuously during the iteration process. This is shown in figure 6.5a, where a lower negative pore pressure ($\Delta u_{t+0}$) is obtained in the top layer and is believed to be the reason that a faster consolidation process is obtained in the numerical model. Furthermore, deformations due to stability issues against surrounding ground might also contribute to excess pore pressure.

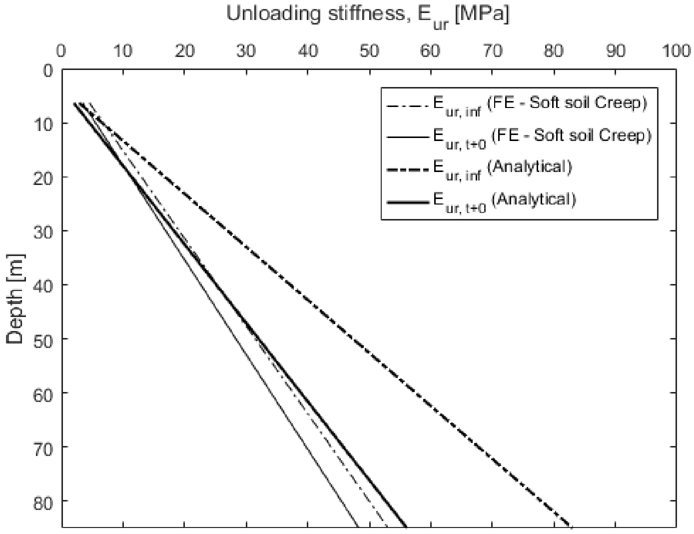


**Figure 6.6:** Unloading stiffness, $E_{ur}$ implemented in the analytical versus numerical model

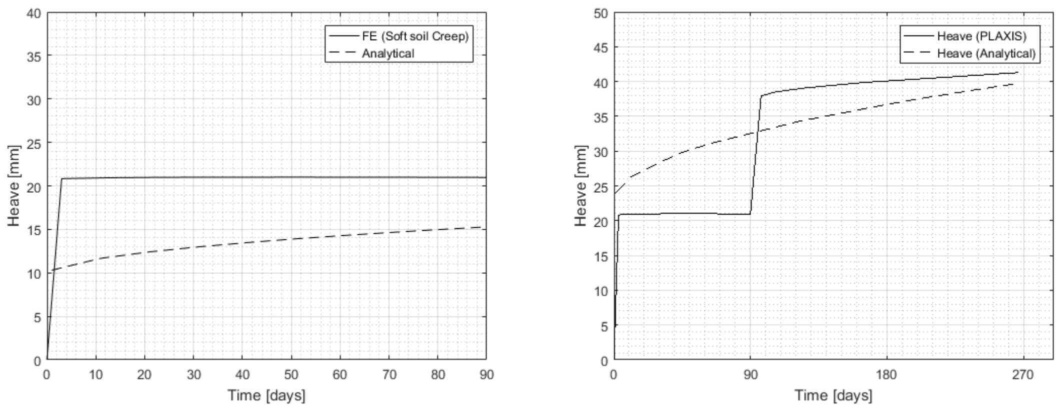


**(a)** Test excavation 3m

**(b)** Main excavation

**Figure 6.7:** Analytical derived estimation of heave versus PLAXIS results, at 22m depth. (Analytical estimated heave with permeability of 5E-10 m/s)

## Numerical results versus field measurements

Results obtained by numerical modelling indicates on lower levels of heave caused by unloading, in comparison with field measurements obtained by Persson (2004), see figure 6.8. As earlier mentioned the magnitude of heave is to some extent difficult to compare with field measurements as the limitations includes the installation of piling. The development of heave beyond construction stage, during the consolidation phases, are thereby more significant. However, it should be highlighted that effects of piling also affects the excess pore pressure development and recovery of the state of pressure in the soil. The obtained states of pressure, during numerical modelling, are thereby lower than what was obtained in field, due to that the positive pore pressure entailed by piling is not taken in consideration, see figure 6.9.

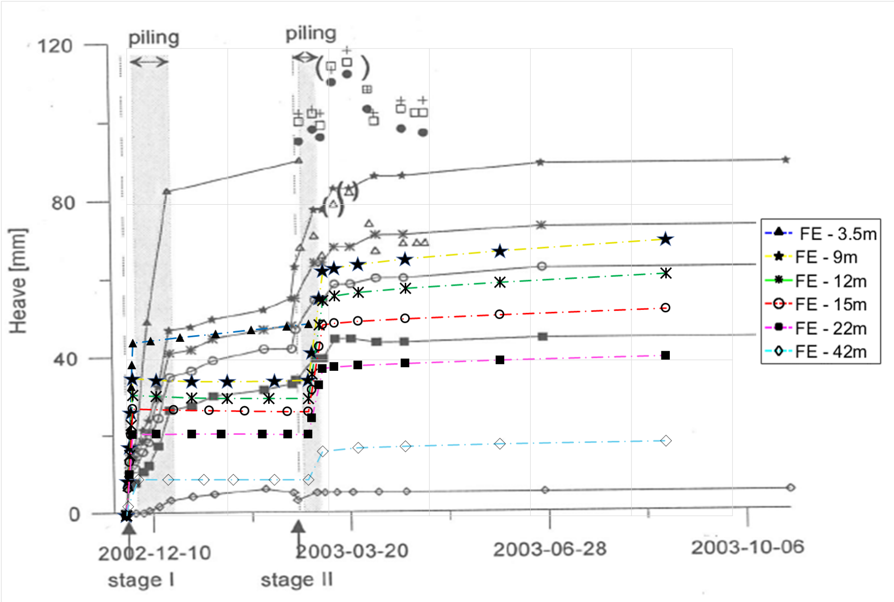


**Figure 6.8:** Comparison of field measurements of heave obtained by Persson (2004) and numerical modelling results

In addition to the fact that the absolute value does not correspond to field measurements, see figure 6.9, it also appears that the created model failed to capture recovery, during the consolidation phases, either. The recovery of pore pressure during both consolidation phases are minor, hence a slow development of heave where obtained. A sensitivity analysis has therefore been conducted with regards to the permeability, in attempt to capture the recovery better and to analyze the impact an adjusted permeability will give on the development of heave, see figure 6.11-6.10. Although, that the permeability in the top 15 meters was adjusted by a factor of 4, the results seen in figure 6.11 indicates on an failed attempt to resemble the recovery of state of pore pressure.

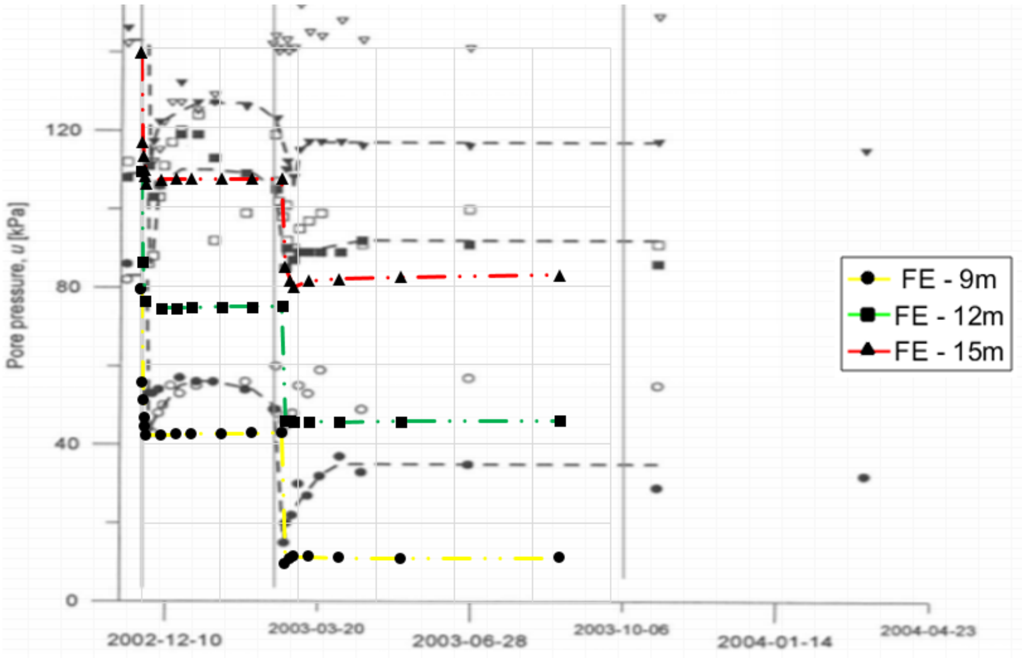


**Figure 6.9:** Comparison of field measurements of pore pressure obtained by Persson (2004) and numerical modelling results

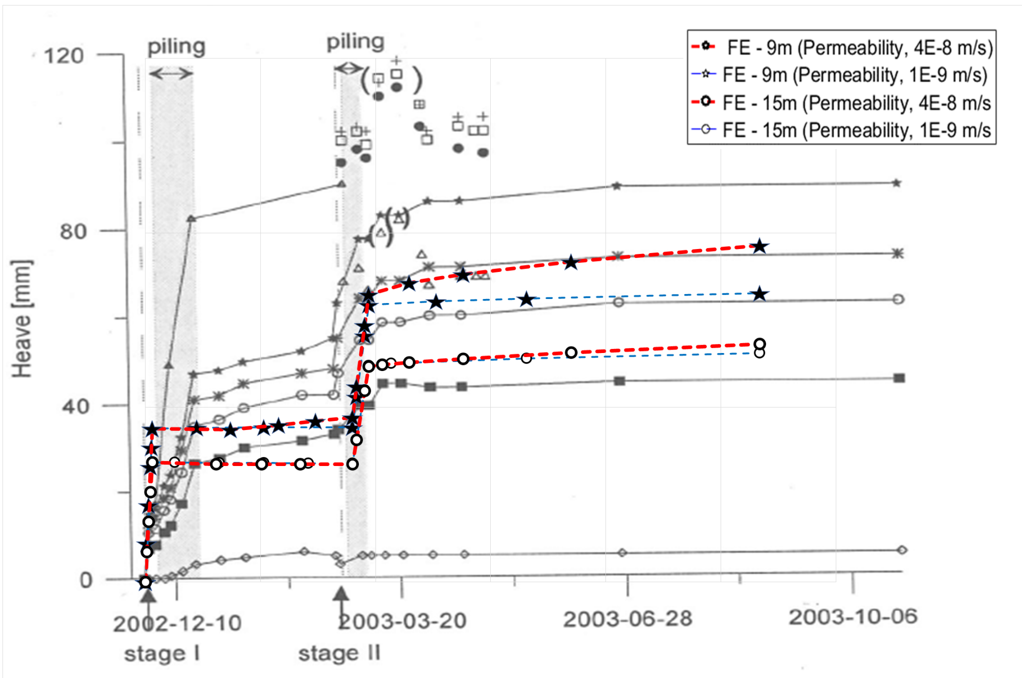


**Figure 6.10:** Sensitivity analysis with regards to permeability (Heave versus time).

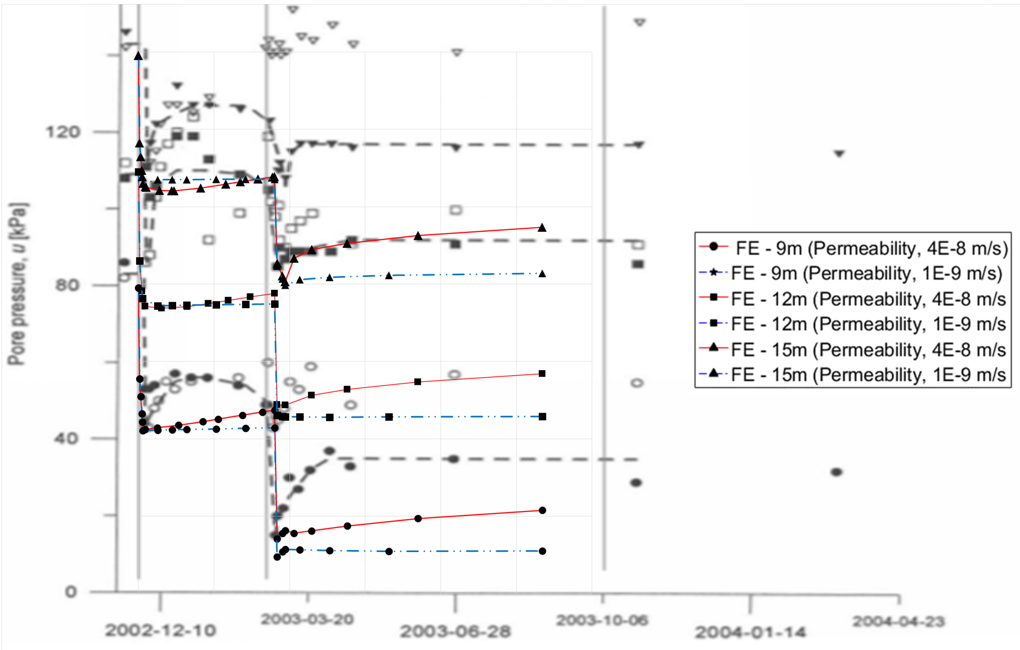


**Figure 6.11:** Sensitivity analysis with regards to permeability (Pore pressure versus time).

# 7
# Discussion

As constitutive models only capture certain features of soil behavior, approximations and set up based on assumptions, the quality of the results relies exclusively on the model set up. Within this chapter, a discussion appears regarding the validity of the model and results, where-after it proceeds to address the main questions forming the scope of this thesis, presented in Chapter 1.2.

## Validity of the model, results and sensitivity analysis

By performance of an analytical evaluation of the stress- and pore-pressure distribution in the soil, but also their changes with respect to time, an additional validation method was created , in addition to field measurements, for the numerical model. The analytical evaluation was thus used as a complement to the calibration procedures, and served as a guideline during the model set-up. Despite the evaluation of soil parameters from laboratory tests (e.g. CRS, triaxial and oedometer), they were subjected to further calibration in attempt to capture the field measurements. However, it should be noted that difficulties was encountered during calibration since the chosen material model fails to capture the stress-strain relationship and stress path of the soil in particular during extension, see figure 6.3-6.4. The underlying reason for the difficulty of capturing the extension behavior is believed to be the lack of incorporation of behaviors such as anisotropy, small strain stiffness and destructuration. By inclusion of anisotropy, the yield surface is represented by a sheared ellipse, in the p'q-plane, and the actual soil behaviour would thereby be resembled much better. Furthermore, effects as a result of incorporation of anisotropy would have contributed to an better coherence during compression as well as extension stress-paths, and incorporation of small-strain stiffness would have lead to less heave.

By performance of a sensitivity analysis with regards to permeability, see figure 6.11, it could be concluded that an increase of permeability would affect the recovery of the pore pressure. However, in order for the water pressure to begin to show a more consistent behavior in comparison with field measurements, an increase in permeability was required by at least a factor of 40. Thus, such an adjustment requires that you reflect on the validity of such an assumption. The validity of such an assumption might therefore be arguable, however previous studies shows tendencies in cracking in the top layer (10-15 meters) of clay with increased permeability, as high as 5E-8 m/s, as a consequence (Berntson, 1983). However, the question arises regarding how long it takes for cracking to form, and thereby if the analyzed time is sufficient for such behavior. Furthermore, it is perhaps more likely that minor in-

termediate layers of permeable material (i.e. sand, silt or silty clay) may be present in the clay, leading to a higher macro permeability of the clay compared to what is measured in soil samples in the lab. In such case, the excess pore pressure will dissipate much faster than presented in the analytical and numerical analysis and results from the field measurements would thereby agree better. However, if an attempt to resemble the progress of dissipation of excess pore pressure solely, by adjustment of the permeability, it would have led to consequences in terms of increased heave during the analyzed period. Hence, an unreasonable magnitude may have been obtained, which would have indicated that the applied unloading modulus in the numerical model is too low.
The previous argument regarding a more advanced material model becomes even more relevant, as incorporation of bonding and degradation of for example small-strain stiffness would "counteract" the development of heave during the analyzed period due to an increase in permeability. But since an analysis of such kind (that is, with a material model also incorporating effects of anisotropy and small-strain stiffness) have not been conducted within the framework of this thesis, the effects it would have on our results can only be considered as speculative so far and therefore should be investigated further in research.

Furthermore, distinction of heave caused by piling or excavation, obtained by field measurements, has not been performed due to the limitations of this thesis. The piling does not only contribute to positive excess pore pressure, which counteracts the negative pore pressure caused by unloading, but it also contributes to heave caused and driven by factors excluded from the analysis due to the scope of this study. Also, it is difficult to separate the contribution to heave and possibly also shear induced excess pore water pressures in the excavation that may have been caused by mobilization of shearing/slope stability due to the higher level of the surrounding ground.

## Suitability of the chosen model and the importance of incorporation of viscous effects

Although, neither the parameters nor the absolute values of the developed heave might be fully correct for the study case, the focus should be on the long-term performance and the obtained behavior of the soil in the numerical model in comparison with field surveys. As earlier mentioned, the material model (Soft soil Creep) was not able to capture the response of the field measurements from Götatunneln L3 (Persson, 2004). The SSC model also showed difficulty of calibrating the soil behavior against extension, while the model proved to be more appropriate in calibration against compression. Additionally, the material model failed to resemble the dissipation of pore pressure measured in the field. This is believed to be the reason why, in the analysis, a minor part of the obtained heave were developed during the consolidation phases, see figure 6.8. In case of a more realistic resemblance of the recovery of pore pressure a smoother development of heave would have been obtained.

Prevailing soil characteristics naturally changes when subjected to stress and strain changes, and the permeability and stiffness are of such factors. For accurate prediction of the consequences followed by excavation, a more advanced model, which incorporates viscous effects in combination with behaviors such as anisotropy, small-strain stiffness and destructuration is therefore required. Incorporation of viscous effects is essential when analyzing the long-term performance of areas with on-going and potential future creep rates which is the case with the construction of the Götatunnel. However, it should be clarified that a more advanced model entails higher requirements on the evaluated parameters, which often means more time-consuming analyses. Additionally, implementation of advanced models sets requirements on deeper knowledge in the area and also validation of such "new" advanced models against lab. test data as well as field/case studies.

When comparing the unloading modules retrieved from the analytical versus the numerical model, see figure 6.6, a distinct difference appears. The unloading modulus implemented in the analytical model, based on equation 2.6 presented by Trafikverket (2016), takes the unloading modulus presented by (Persson, 2004) in account. The modulus obtained from the formula implements a higher modulus in comparison with the numerical model which derives the soil stiffness from the available laboratory tests. The impact a higher modulus have on the result were therefore analyzed, see figure 5.3 and it appears that a higher modulus contributes to a lower instant heave development and a faster consolidation (dissipation of negative excess pore pressures). Since previous research has resulted in various of relations for deriving the unloading modulus of soil, the question thereby arises regarding which unloading modulus should be implemented in order to calibrate the model. Furthermore, it becomes more relevant given that research has proven that a deviation is obtained between the unloading modulus derived by laboratory testing in comparison with what can be found in field. The deviations are believed to depend partly on the impact sampling has on the soil, but also the difficulty of recreating the in-situ conditions of the soil sample within a laboratory. Also, boundary effects such as possible on-going creep settlements in the area surrounding the excavation may lead to less heave in the field. This further emphasizes the importance of incorporation of viscous effects, since the acting deformations followed by ongoing creep rates is considered to represent a state of loading. It can thus be stated that, in particular in cases with on-going creep settlements in the field, it may be difficult with current sampling and laboratory methods to obtain modulus values that represents values found in field. As always, one should consider the limitations and differences between the boundary conditions in the lab compared to those present in the field.

# 8
# Conclusion

Based on the study conducted in this thesis, the material model Soft soil Creep has proven to be inadequate of describing soil behaviour especially for the available triaxial extension tests and thereby the unloading behaviour. The difficulties during resemblance of the extension tests are the main reason for this conclusion, followed by the failure to resemble the dissipation of excess pore pressure. However, the field measurements may have been influenced of installation of concrete piles in adjacent areas, as well as mobilization of stability/shear forces due to the surrounding higher ground surface. Based on this work, it can be concluded that a more advanced material model that implements behaviors, such as anisotropy, small-strain stiffness and destructuration, may be needed to resemble the pore water dissipation, and obtain a better prediction regarding the stress paths and stiffness of the soil as compared to what was measured in the lab. This, in order to be able to resemble the soil behavior more accurately. Furthermore, it could be concluded that the implementation of a material model that also incorporates viscous effects is essential to analyze the short and long-term performance of constructions, and the effects on the sorrounding, in soft soils with on-going creep deformations.

The implementation of equation 2.6, presented by Trafikverket (2016), has proven to deliver reasonable results. Given that it is based on field measurements by Persson (2004) and soil samples collected within the study area of this thesis, it is logical. However, although the unloading modulus according to 2.6 did not cohere with the laboratory tests, it could not be rejected since the material model has proven to be unsuitable for such problems. In order to make a justified evaluation of the suitability of equation 2.6, further studies, implementing a more advanced material model, should be conducted.

There is currently no commercially available model considering for example rate-dependency, anisotropy and small strain stiffness. Research is on-going at Chalmers to further develop an existing rate-dependent model that already incorporates anisotropy and destructuration. Additional features that needs to be incorporated are the small-strain stiffness in loading and unloading stress paths. Development of such a model should be stressed, since it may result in improved predictions.

# References


Alén, C., & Jendeby, L. (1996). Hävning vid avschaktning-ullevi, ett praktikfall, in ‘. *NGM-96, Reykjavik, Island*, 353–358.

Assouline, S., & Or, D. (2006). Anisotropy factor of saturated and unsaturated soils. *Water resources research*, *42*(12).

Basma, A. A., Al-Homoud, A. S., Malkawi, A. I. H., & Al-Bashabsheh, M. A. (1996). Swelling-shrinkage behavior of natural expansive clays. *Applied Clay Science*, *11*(2-4), 211–227.

Berntson, J. A. (1983). *Portrycksvariationer i leror i göteborgsregionen.* Gothenburg: Department of GeoEngineering, Chalmers University of Technology.

Brinkgreve, R., & Vermeer, P. (1998). Plaxis manual. *Version*, *7*, 5–1.

Brinkgreve, R. B. (2005). Selection of soil models and parameters for geotechnical engineering application. In *Soil constitutive models.* doi: 10.1061/40771(169)4

Brinkgreve, R. B., Kumarswamy, S., & Swolfs, W. (2017). Material models manual [Computer software manual].

EN, B. (1997). 1 (2004). eurocode 7: Geotechnical design-part 1: General rules. *British Standards, UK*.

Fredlund, D. G., & Hasan, J. U. (1979). One-dimensional consolidation theory: unsaturated soils. *Canadian Geotechnical Journal*, *16*(3), 521–531.

Friis, Å., & Sandros, C. (1994). *Hävning vid stora schakter i lera : Ullevi - ett praktikfall.* (Master thesis)

Infrastruktur, K. (2005). *En kortkurs om triaxialförsök på främst normalkonsoliderade och svagt överkonsoliderade leror* (Tech. Rep.). Gothenburg: Chalmers Tekniska Högskola.

Jia, J. (2018). *Soil Dynamics and Foundation Modeling Offshore and Earthquake Engineering.* Cham: Springer International Publishing.

Jonsson, J., & Kristiansson, A. (2004). *Massundanträngning i samband med pålning i lera.* Chalmers tekniska högsk.

Karlsrud, K., & Hernandez-Martinez, F. G. (2013). Strength and deformation properties of norwegian clays from laboratory tests on high-quality block samples. *Canadian Geotechnical Journal*, *50*(12), 1273–1293.

Karstunen, M., & Amavasai, A. (2017). *BEST SOIL : Soft soil modelling and parameter determination* (No. July).

Karstunen, M., Wiltafsky, C., Krenn, H., Scharinger, F., & Schweiger, H. F. (2006). Modelling the behaviour of an embankment on soft clay with different constitutive models. *International Journal for Numerical and Analytical Methods in Geomechanics*, *30*(10), 953–982. doi: 10.1002/nag.507

Kempfert, H.-G., & Gebreselassie, B. (2006). *Excavations and foundations in soft soils.* Springer Science & Business Media.

Knappett, J., & Craig, R. F. (2012). *Craig's soil mechanics* (8th ed. ed.). Abingdon, Oxon: Spon Press.

Larsson, R. (1986). *Consolidation of soft soils* (Tech. Rep.). Linköping: Swedish Geotechnical Institute.

Mesri, G., Ullrich, C., & Choi, Y. (1978). The rate of swelling of overconsolidated clays subjected to unloading. *Géotechnique*, *28*(3), 281–307.

Persson, J. (2004). *The unloading modulus of soft clay: a field and laboratory study.* Gothenburg: Department of GeoEngineering, Chalmers University of Technology.

Rankka, K., Andersson-Sköld, Y., Hultén, C., Larsson, R., Leroux, V., & Dahlin, T. (2004). Quick clay in sweden. *Swedish Geotechnical Institute Report*, *65*(1), 145.

Runesson, K., Steinmann, P., Ekh, M., & Menzel, A. (2006). Constitutive modeling of engineering materials—theory and computation. *Volume I General Concepts and Inelasticity*.

Schanz, T., Vermeer, P., & Bonnier, P. (1999). The hardening soil model: formulation and verification. *Beyond 2000 in computational geotechnics*, 281–296.

Sweco. (2014). *PM Geoteknik, Västlänken Station Centralen, Geoteknisk utredning för detaljplan* (Vol. 46; Tech. Rep. No. 556507). Gothenburg: n/a.

Ti, K. S., Gue See, S., Huat, B. B., Noorzaei, J., & Saleh, M. (2009). A Review of Basic Soil Constitutive Models for Geotechnical Application. *Electronic Journal of Geotechnical Engineering*, *14*, 18.

Tornborg, J. (2017). *Svälltryck På Grund Av Avlastning I Lös Lera* (Tech. Rep.). Gothenburg: Svenska Bygg branschens Utvecklingsfond.

Trafikverket. (2016). *Trafikverkets tekniska råd för geokonstruktioner - TR Geo 13* (Tech. Rep.). Author.

Vermeer, P., & Neher, H. (1999). A soft soil model that accounts for creep. In *Proceedings of the international symposium "beyond 2000 in computational geotechnics* (pp. 249–261).

Waterman, D., & Broere, W. (2004). Practical application of the soft soil creep model. *Plaxis Bulletin*, *15*.

Won, J. (2013). Anisotropic strength ratio and plasticity index of natural clays. In *Proceedings of the 18th international conference on soil mechanics and geotechnical engineering, icsmge* (pp. 2–6).

Wood, T. (2016). *On the small strain stiffness of some scandinavian clays and impact on deep excavation.* Chalmers University of Technology.

Yuan, J., & Nguyen, H. V. (2011). Laboratory study on soil shear stiffness and strength under unloading conditions. *Journal of Testing and Evaluation*, *39*(5), 821–830.

Yu-qi, L., Hong-wei, Y., & Kang-he, X. (2005). On the dissipation of negative excess porewater pressure induced by excavation in soft soil. *Journal of Zhejiang University-SCIENCE A*, *6*(3), 188–193.

Zaslavsky, D., & Rogowski, A. (1969). Hydrologic and morphologic implications of anisotropy and infiltration in soil profile development 1. *Soil Science Society* *of America Journal*, *33*(4), 594–599.

Zeevaert, L. (1983). *Foundation engineering for difficult subsoil conditions* (2. ed. ed.). New York: Nostrand Reinhold.

Zhang, Y. G., Zhang, K. Y., Li, W. L., & Shi, Q. Z. (2011). Unloading triaxial experimental study on stress path of excavated soil slope. In *Advanced materials research* (Vol. 243, pp. 2797–2801).

# A
# Appendix

**Table A.1:** Calibrated parameters and data for respective soil layer in PLAXIS 2D

| - | Fill | Soil layer 1 | Soil layer 2 | Soil layer 3 | Soil layer 4 | Soil layer 5 |
|---|---|---|---|---|---|---|
| Soil layer depth | 0 - 3 m | 3 - 10 m | 10 - 15 m | 15 - 50 m | 50 - 70 m | 70 - 85 m |
| Material model | Linear elastic | Soft soil creep | Soft soil creep | Soft soil creep | Soft soil creep | Soft soil creep |
| drainage type | Drained | Undrained | Undrained | Undrained | Undrained | Undrained |
| $\gamma_{unsat}$ | 16 | 16.3 | 15.7 | 16.4 | 16.8 | 17.8 |
| $\gamma_{sat}$ | 16 | 16.3 | 15.7 | 16.4 | 16.8 | 17.8 |
| void ratio | 0.5 | 1.74 | 2.18 | 1.7 | 1.57 | 1.3 |
| E' | 30E3 | - | - | - | - | - |
| v' | 0.333 | - | - | - | - | - |
| $\lambda^*$ | - | 0.16 | 0.21 | 0.22 | 0.3 | 0.22 |
| $\kappa^*$ | - | 0.023 | 0.02 | 0.013 | 0.02 | 0.0165 |
| $\mu^*$ | - | 7.7E-3 | 7.9E-3 | 7.8E-3 | 7.1E-3 | 5.4E-3 |
| $c'_{ref}$ | - | 1.3 | 1.3 | 1.3 | 1.3 | 1.3 |
| $\phi'$ | - | 32 | 32 | 32 | 32 | 32 |
| $\psi'$ | - | 0 | 0 | 0 | 0 | 0 |
| Data set | Standard | standard | standard | standard | standard | standard |
| - type | - | Very fine | Very fine | Very fine | Very fine | Very fine |
| flow parameter, $k_x$ | 0.6 | 0.0864E-3 | 0.0864E-3 | 0.0432E-3 | 0.0432E-3 | 0.0432E-3 |
| flow parameter, $k_y$ | 0.6 | 0.0864E-3 | 0.0864E-3 | 0.0432E-3 | 0.0432E-3 | 0.0432E-3 |
| permeability, $c_k$ | 1000E12 | 1000E12 | 1000E12 | 1000E12 | 1000E12 | 1000E12 |
| strength | - |  | Rigid | Rigid | Rigid | Rigid |
| Rigid |  |  |  |  |  |  |
| $k0$ determination | Automatic | Automatic | Automatic | Automatic | Automatic | Automatic |
| OCR | - | 1.76 | 1.69 | 1.66 | 1.33 | 1.3 |
| POP | - | 0.0 | 0.0 | 0.0 | 0.0 | 0.0 |

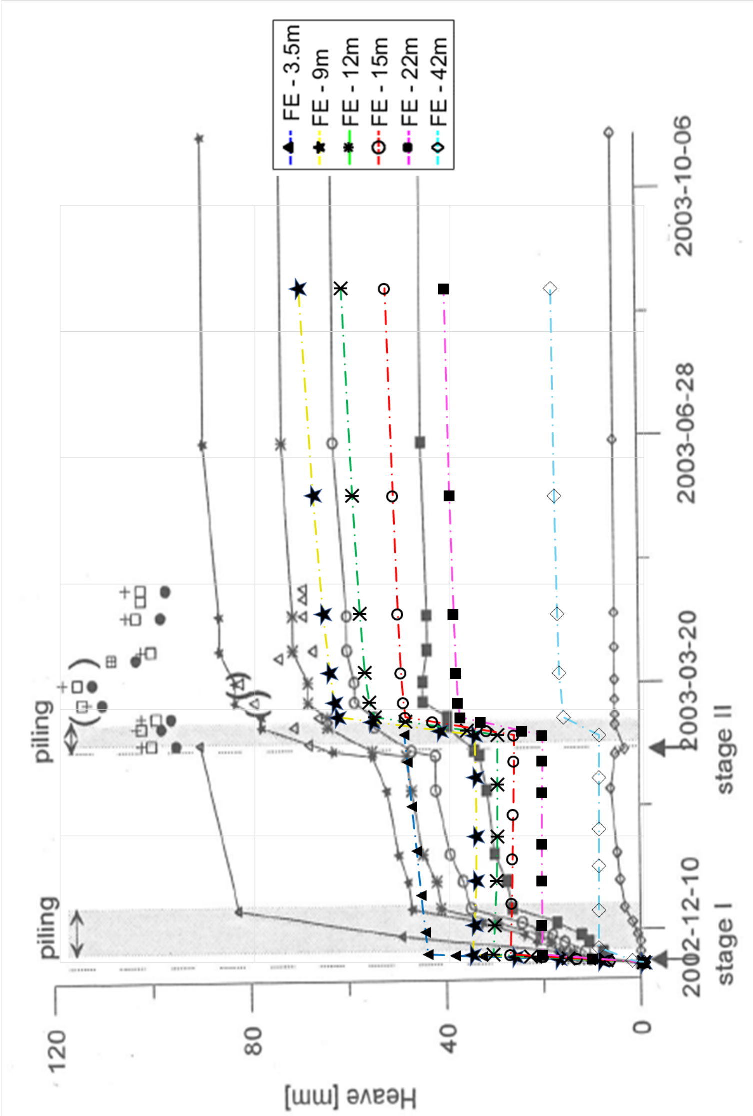


**Figure A.1:** Comparison of field measurements of heave obtained by Persson (2004) and numerical modelling results

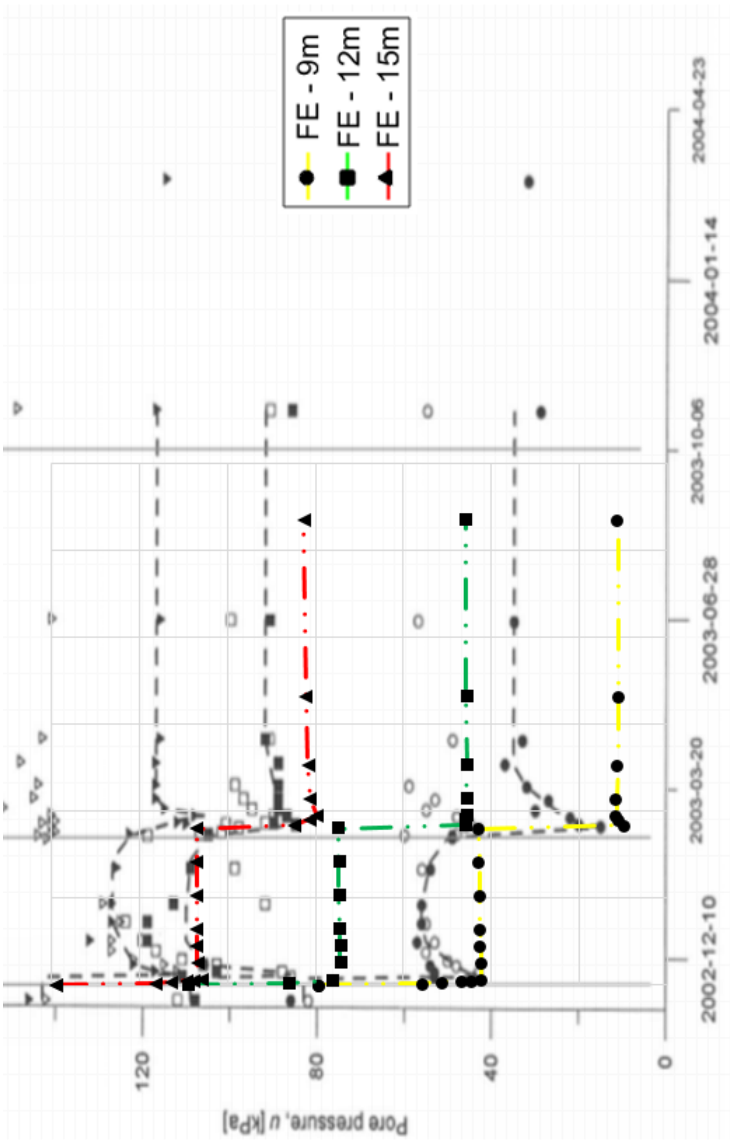


**Figure A.2:** Comparison of field measurements of pore pressure obtained by Persson (2004) and numerical modelling results

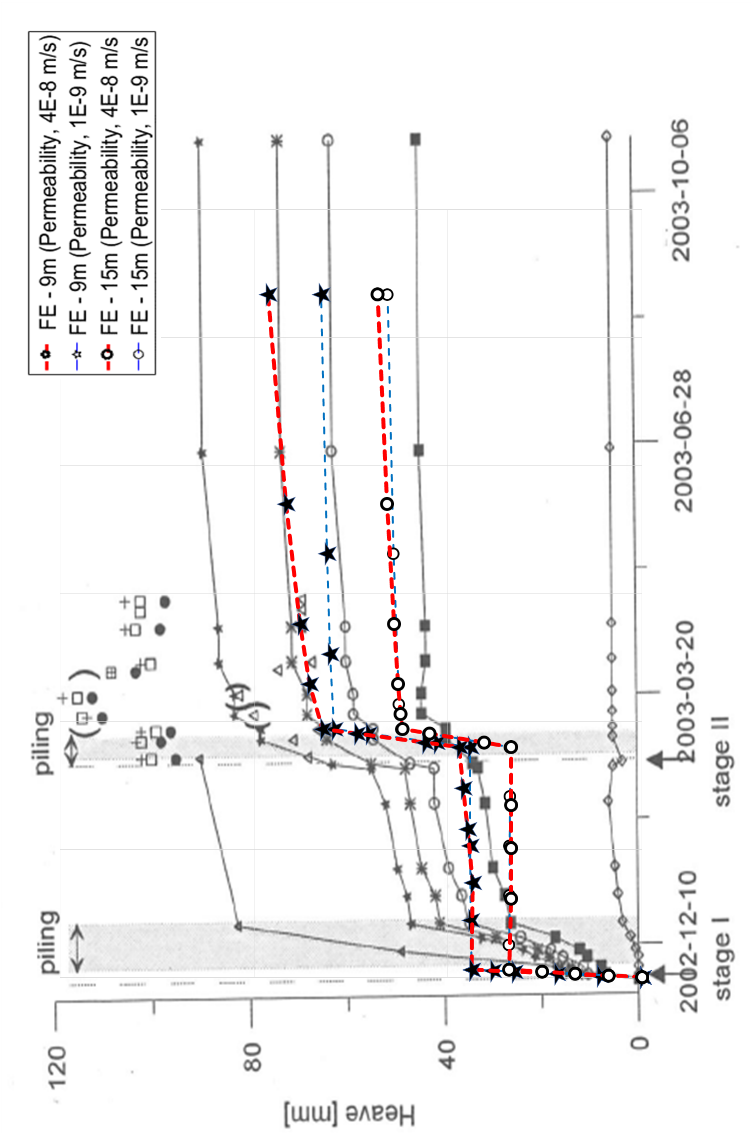


**Figure A.3:** Sensitivity analysis with regards to permeability (Heave versus time).

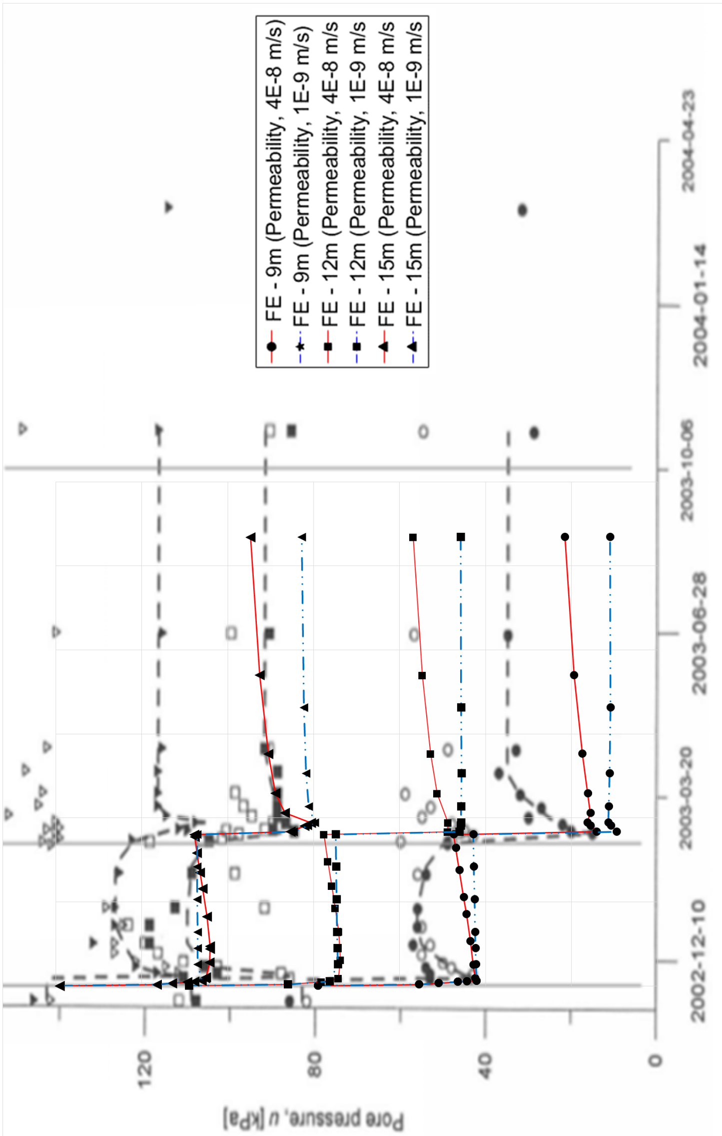


**Figure A.4:** Sensitivity analysis with regards to permeability (Pore pressure versus time).